

U–Pb evidence of ~ 1.7 Ga crustal tectonism during the Nimrod Orogeny in the Transantarctic Mountains, Antarctica: implications for Proterozoic plate reconstructions

John W. Goodge ^a, C. Mark Fanning ^b, Vickie C. Bennett ^b

^a *Department of Geological Sciences, Southern Methodist University, Dallas, TX, 75275-0395 USA*

^b *Research School of Earth Sciences, The Australian National University, Mills Road, Canberra, ACT 0200, Australia*

Received 9 August 2000; accepted 13 April 2001

Abstract

The Pacific margin of East Antarctica records a long tectonic history of crustal growth and breakup, culminating in the early Paleozoic Ross Orogeny associated with Gondwanaland amalgamation. Periods of older tectonism have been proposed (e.g. Precambrian Nimrod and Beardmore Orogenies), but the veracity of these events is difficult to document because of poor petrologic preservation, geochronologic uncertainty due to isotopic resetting, and debated geological field relationships. Of these, the Nimrod Orogeny was originally proposed as a period of Neoproterozoic metamorphism and deformation within crystalline basement rocks of the Nimrod Group, based on ~ 1000 Ma K–Ar mineral ages. Later structural and thermochronologic study attributed major deformation features in the Nimrod Group to Ross-age basement reactivation. Yet, new SHRIMP ion microprobe U–Pb zircon age data for gneissic and metaigneous rocks of the Nimrod Group indicate a period of deep-crustal metamorphism and magmatism between ~ 1730 – 1720 Ma. Igneous zircons from gneissic Archean protoliths show metamorphic overgrowths of ~ 1730 – 1720 Ma, and an eclogitic block preserved within the gneisses contains zircons yielding an average metamorphic crystallization age of ~ 1720 Ma. Deformed granodiorite that intrudes the gneisses and associated metasedimentary rocks yields a concordant zircon crystallization age of ~ 1730 Ma. Despite scant petrologic evidence for these metamorphic and igneous events, the zircon ages from these diverse rock types indicate major crustal thickening, possibly due to collision, in the late Paleoproterozoic. We therefore recommend revival of the term Nimrod Orogeny to describe Paleoproterozoic tectonic events in rocks of the East Antarctic shield. Similarities in the ages of igneous and metamorphic events in the Nimrod Group and geologic units elsewhere in present-day East Antarctica, southern Australia and southwestern North America suggest they may have played a role in early supercontinent assembly. In particular, similarity with the Laurentian Mojave province is consistent with Proterozoic plate reconstructions joining ancestral East Antarctica with western Laurentia. © 2001 Elsevier Science B.V. All rights reserved.

Keywords: Paleoproterozoic; Antarctica; Orogeny; Geochronology

* Corresponding author. Tel.: +1-214-7684140; fax: +1-214-7682701.

E-mail address: jgoodge@mail.smu.edu (J.W. Goodge).

1. Introduction

The East Antarctic shield, representing one of the oldest cratonic elements on Earth, is mostly covered by the modern polar ice cap. Although coastal outcrops around much of East Antarctica show a long record of geologic events spanning the early Archean to Neoproterozoic, extensive exposures in the Transantarctic Mountains reveal little of its Precambrian ancestry. Crustal thickness and geophysical patterns reveal that this mountain belt marks the Pacific edge of the East Antarctic shield, leaving little doubt that the Transantarctic Mountains are underlain by crystalline basement. However, most of the mountain belt exposes late Neoproterozoic to mid-Mesozoic sedimentary and volcanic sequences, and Precambrian cratonic events documented elsewhere in the East Antarctic shield are not recorded. In addition, widespread deformational and magmatic effects of the ~500 Ma Ross Orogeny are sufficiently strong in most areas to obscure any record of earlier events. These in turn have been modified locally by Cenozoic extension. Because of these factors, evidence of Precambrian geologic events in the Transantarctic Mountains has been difficult to establish with certainty.

Early workers in the Ross Sea region (Fig. 1) recognized unusually high-grade metamorphic rocks in the upper Nimrod Glacier area that appeared on the basis of petrologic and structural relations to be Precambrian in age (Grindley et al. 1964; Grindley, 1972). This high-grade metamorphic complex, the Nimrod Group, contrasts strongly with adjacent sedimentary sequences in terms of lithology, metamorphism, and deformation. Grindley and Laird (1969) defined the Nimrod Orogeny as a period of Precambrian deformation and high-grade metamorphism prevalent in crystalline rocks of the Nimrod Group that is not observed in adjacent sedimentary units. On the basis of K–Ar mineral ages, Grindley and McDougall (1969) suggested that this orogeny was late Precambrian in age (~1000 Ma). Adams et al. (1982) obtained a similar range of Neoproterozoic to early Paleozoic K–Ar ages from Nimrod Group samples, but they attributed the older ages in part to the incorporation of

excess argon in amphibole. Using $^{40}\text{Ar}/^{39}\text{Ar}$ methods, Goode and Dallmeyer (1992, 1996) confirmed that the previously reported Proterozoic K–Ar ages were unreliable due to excess argon. They reported metamorphic mineral cooling ages of 525–490 Ma, showing that regional, high- T mineral recrystallization and fabric development within the Nimrod Group occurred during the Ross Orogeny. U–Pb ages from metasedimentary and metaigneous rocks showed further that major metamorphic and deformational events recorded by the Nimrod Group occurred during Ross time (Goode et al. 1993a,b). Therefore, the dominant preserved deformation features, metamorphic assemblages, and mineral cooling ages in these crystalline rocks record a high- T , high- P , and high strain response to Ross orogenic events, and they are not a signature of Precambrian orogenesis as suggested by others (Grindley and Laird, 1969; Grindley, 1972).

Despite the extensive Ross overprinting, the Nimrod Group does retain cryptic evidence of Precambrian activity. Sm–Nd isotopic data and U–Pb ages from igneous and detrital zircons in the Nimrod Group indicate an Archean to Paleoproterozoic history (Borg et al. 1990; Walker and Goode, 1991; Bennett and Fanning, 1993). Recent U–Pb dating of zircons by sensitive high-resolution ion microprobe (SHRIMP) has further clarified the history of the Nimrod Group (Goode and Fanning, 1999), showing that its protoliths include ~3.0 Ga magmatic rocks that were affected by a series of Proterozoic and early Paleozoic thermotectonic events. As a means of re-evaluating the older history in the Nimrod Group, we analyzed samples from several high-grade lithologies with apparently complicated deformational and metamorphic histories in order to recover information about possible Precambrian events. Here, we present new SHRIMP U–Pb analyses of zircons from layered gneiss, eclogite, and metaplutonic rocks that reveal a common record of ~1730–1720 Ma orogenic activity. The coeval crustal metamorphism, eclogite formation, and magmatism, documented here, indicate a period of major, deep-seated orogenesis in this region, although nearly all petrologic and structural evidence for these Paleoproterozoic

metamorphic and magmatic events has been obliterated by Ross tectonism. We suggest that the term Nimrod Orogeny, previously questioned as a geologically recognizable event (Goodge and Dallmeyer, 1996), be revived to cover the ~ 1.7 Ga metamorphic and magmatic events described here.

2. Geologic setting

The Nimrod Group is exposed in the region of the upper Nimrod Glacier (Fig. 1). Here, high-grade Nimrod metamorphic rocks occur in the Miller and Geologists ranges, inboard of low-grade Neoproterozoic to lower Paleozoic sedimentary rocks and a regional ~ 500 Ma granitic batholith complex. As described elsewhere, the Nimrod Group is a heterogeneous assemblage of gneisses, schists and orthogneisses, including banded quartzofeldspathic to mafic gneiss, pelitic schist, quartzite, amphibolite, granitic to gabbroic orthogneiss, migmatite, calc-silicate gneiss, marble, relict eclogite and pods of ultramafic rocks (Grindley et al., 1964; Grindley, 1972; Goodge et al., 1993a; Peacock and Goodge, 1995). The Nimrod Group preserves pervasive ductile tectonite fabrics recording mid-crustal Ross deformation (Goodge et al., 1993a) and is intruded by post-tectonic Late Cambrian to Early Ordovician granitoid plutons (Gunner, 1976; Borg et al., 1990).

Existing Nimrod Group age data reveal a Precambrian history overprinted by younger Ross events. From layered gneisses and schists, U–Pb zircon ages of 3290–3060 Ma (Bennett and Fanning, 1993; Goodge and Fanning, 1999), as well as whole-rock Nd-model ages of 3.10–2.72 Ga and $\varepsilon_{\text{Nd}}(0)$ values of -33 to -28 (Borg et al., 1990; Borg and DePaolo, 1994), suggest crust formation initially occurred in the Middle to Late Archean. Igneous and metaigneous rocks range from strongly deformed orthogneisses and syn-tectonic bodies to undeformed post-tectonic plutons. A tectonized granodiorite orthogneiss that cross-cuts the layered gneisses noted above yielded a 1.73 Ga $^{207}\text{Pb}/^{206}\text{Pb}$ age (Bennett and Fanning, 1993) and a 2.73 Ga Nd-model age (Borg et al., 1990). This discordant orthogneiss

reflects Paleoproterozoic magmatism by localized partial melting, or at least partial assimilation, of pre-existing crust. Syn-tectonic intrusive units yielded U–Pb ages between 540–520 Ma (Goodge et al., 1993b), whereas large post-tectonic plutonic bodies are 500–475 Ma (Gunner and Mattinson, 1975; Gunner, 1976). Detrital zircons from a Nimrod Group quartzite yielded U–Pb ages ranging from 2555 Ma to 1734 Ma (Walker and Goodge, 1991), compatible with a Late Archean to Paleoproterozoic East Antarctic provenance (Tingey, 1991). $^{40}\text{Ar}/^{39}\text{Ar}$ cooling ages from muscovite and hornblende, and U–Pb ages from monazite and zircon, indicate that the latest metamorphism occurred between ~ 550 –520 Ma (Goodge and Dallmeyer 1992, 1996; Goodge et al. 1993b). These young ages, obtained from minerals comprising high- T tectonite fabrics, reflect Ross-age basement orogenic activity. As noted above, the dynamothermal features once ascribed to a Precambrian ‘Nimrod’ Orogeny (Grindley and Laird, 1969; Grindley, 1972) are now recognized as the response of cratonic basement to latest Neoproterozoic and early Paleozoic plate-margin tectonism.

3. SHRIMP U–Pb zircon results

In this paper, we discuss SHRIMP U–Pb zircon age results from four samples collected from the Nimrod Group in the Miller Range (Figs. 1 and 2). These include two samples of layered gneiss (samples 85-20H and 89-65A), a relict eclogite tectonic block (sample 90-131A), and a granodiorite orthogneiss unit (sample M-28). We present new U–Pb data for samples 89-65A, 90-131A and M-28 (Tables 1, 4 and 5) and summarize data for sample 85-20H (Table 2), previously discussed by Goodge and Fanning (1999). Here we focus on zircons yielding ~ 1730 –1720 Ma ages, but Nimrod gneisses reveal additional evidence for igneous and metamorphic events at ~ 3000 , ~ 2900 , ~ 2500 , and ~ 530 Ma (Goodge and Fanning, 1999).

For samples 89-65A, 90-131A and M-28, zircons were separated using standard heavy-liquid and magnetic methods, and hand picked to obtain

a representative selection of all components present in the zircon population. Zircon grains were mounted in an epoxy disk together with grains of Sri Lanka reference zircon SL-13 for U concentration and Duluth Gabbro reference zircon AS-3 for U–Pb calibration (Paces and Miller, 1993). The zircon grains were sectioned approximately in half and polished, and images were obtained by both optical microscopy and cathodoluminescence (CL) on a scanning electron microscope (Figs. 3, 6 and 8). With CL imaging, it is possible to distinguish the internal growth

structure of zircons, including igneous and metamorphic crystallization textures, resorption surfaces, and overgrowths (e.g. Vavra, 1990; Schaltegger et al., 1999). We analyzed 20 μm areas that were optically clear, crack free, and represented single domains as observed in CL images. The zircons were analyzed using SHRIMP II at the Research School of Earth Sciences, The Australian National University, under standard operating conditions (Compston et al. 1992; Williams, 1998). Data reduction procedures and corrections generally follow those outlined by Compston et al. (1992) and Muir et al. (1996). Concordia plots and weighted mean age calculations were made using ISOPLOT/EX (Ludwig, 1999).

For samples 89-65A and 90-131A, individual grains were analyzed as part of a single extended SHRIMP analytical session involving a number of related samples from the Transantarctic Mountains. Most of the analyzed grains have cores with distinct overgrowths that could be analyzed separately, yielding a large number of individual U–Pb ages. The AS-3 standard was analyzed 34 times during the analytical session. Errors for individual analyses are quoted at the 1σ level; however, all age calculations are given with uncertainties as 95% confidence levels. Sample 85-20H was analyzed similarly, as described by Goodge and Fanning (1999). Sample M-28 was analyzed on SHRIMP I, using Sri Lanka reference zircon SL-13 for both U concentration and U–Pb calibration.

3.1. Layered gneisses

Samples 85-20H and 89-65A are banded biotite-hornblende gneisses collected in the west-central Miller Range (location $83^{\circ}09'37''$ S; $155^{\circ}58'$ E), in the vicinity of Camp Ridge (Fig. 1). This locality is characterized by heterogeneous gneiss and schist that host thin, sheet-like, felsic tectonites and that enclose remnant tectonic blocks of eclogite (Grindley et al., 1964; Goodge et al., 1992; Peacock and Goodge, 1995). The layered gneisses and schists (layering on all scales from centimeters to meters) near Camp Ridge include amphibolite, intermediate hornblende-bi-

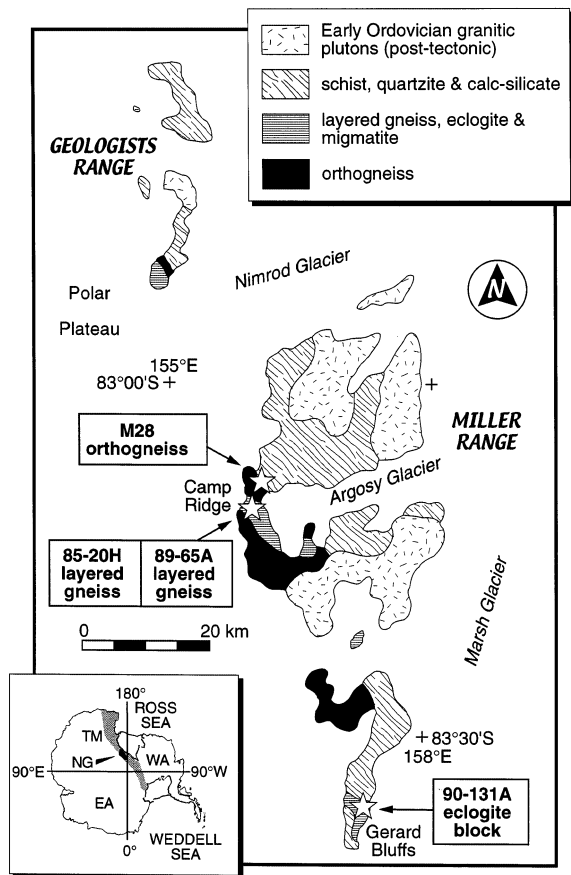


Fig. 1. General geologic map of the Nimrod Group in the Miller and Geologists ranges, central Transantarctic Mountains (simplified from Goodge et al. (1993a)). Stars show locations of samples discussed in this paper. Inset shows location near Nimrod Glacier (NG) in Antarctica. EA East Antarctica; TM Transantarctic Mountains (gray); WA West Antarctica.

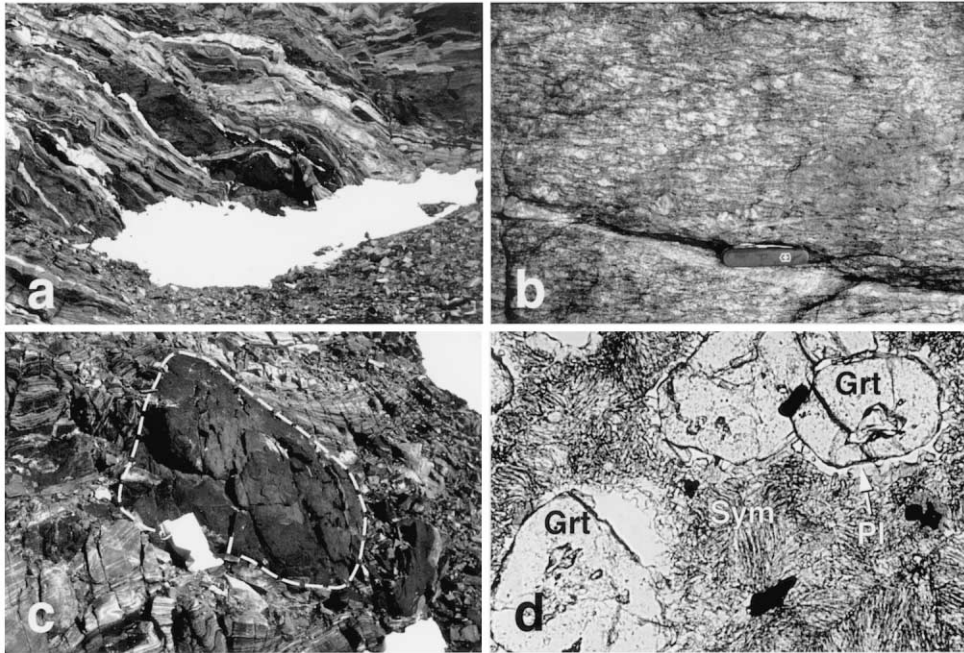


Fig. 2. Photographs of rock units discussed in this paper. (a) Layered gneiss in the Camp Ridge area of the western Miller Range. Note person standing above snow patch for scale. Rock types include intermediate hornblende-biotite gneiss, quartzofeldspathic and pegmatitic gneiss, amphibolite, and garnet-muscovite-kyanite-sillimanite schist. Sample 89-65 is from light-colored quartzofeldspathic gneiss. (b) K-feldspar megacrystic hornblende-biotite orthogneiss from the Camp Ridge area of the western Miller Range, showing tectonite texture similar to that of sample M-28. Note feldspar porphyroclasts and ductile L–S tectonite fabrics (asymmetric with horizontal S, and C planes dipping to left). Knife is 9 cm long. (c) Round eclogite boudin (outlined by white dashed line) in layered gneiss and schist from the Camp Ridge area of the western Miller Range. As in many cases, this mafic block shows a dark rim of amphibolite surrounding a core containing relict eclogite mineral assemblages (see Fig. 2d). Hammer, with sample bag, is 33 cm long. (d) Thin-section photomicrograph of eclogite sample 90-131A, showing anhedral garnet (Grt) rimmed by plagioclase (Pl), and surrounded by symplectite (Sym) intergrowths consisting of low-Na diopsidic clinopyroxene + hornblende + plagioclase + ilmenite + quartz after omphacitic pyroxene. Plane-polarized light. Long dimension of photomicrograph is about 1.2 mm.

otite gneiss, quartzofeldspathic and pegmatitic gneiss, and muscovite-kyanite-sillimanite schist (Fig. 2a). Metamorphic conditions corresponding to the most recent Ross activity in this area were about 700 °C and 8–12 kbar in the upper-amphibolite to lower-granulite facies (Goodge et al., 1992). Sample 85-20H is a coarse-grained gneiss containing quartz, plagioclase, K-feldspar, biotite, and hornblende, with accessory epidote, chlorite, Fe-oxide, sphene, zircon, and apatite. Sample 89-65A is a thin-banded gneiss containing quartz, microcline, plagioclase, biotite and hornblende, with accessory apatite, Fe-oxide, zircon, muscovite, chlorite and epidote. Biotite in both samples is more abundant than hornblende.

Zircons in sample 89-65A show complex internal structures under CL with generally zoned inner areas discordant to secondary rim overgrowths (Fig. 3). Three of the six grains analyzed for the present study (grains 2, 3 and 6) have central areas with oscillatory internal banding and prismatic growth terminations, suggesting primary crystallization of the gneiss protolith from an igneous melt. These cores have embayed margins and truncation of internal growth bands indicating incomplete zircon dissolution or melting after initial crystallization, followed by new zircon growth. The cores of several grains (2 and 3, for example) are overgrown by wide mantles with mottled or sector-zoned texture, and have dark

CL appearance. The grain 2 overgrowth has a prismatic, terminated shape suggesting topotactic growth on an older igneous core (Fig. 3b).

The 12 areas analyzed yielded discordant U–Pb results (Table 1). However, a multi-stage radiogenic Pb-loss history can be postulated for the observed discordant arrays (Fig. 4) that is consistent with the CL interpretation of those areas. The igneous cores have relatively high Th/U ra-

tios (0.58–0.80) and Archean ages; analyses 2.1, 4.1 and 6.1 have $^{207}\text{Pb}/^{206}\text{Pb}$ ages of ~ 3150 Ma and appear to lie along a simple discordia line with an upper concordia intercept at ~ 3180 Ma and a forced lower intercept at ~ 530 Ma (from the weighted mean $^{206}\text{Pb}/^{238}\text{U}$ age for the metamorphic Ross age rims in sample 85-20H). The rim of grain 6 has a $^{207}\text{Pb}/^{206}\text{Pb}$ age of 3015 ± 9 Ma (analysis 6.2, $\sim 3\%$ discordant), but it lies near a discordia line joining ~ 2975 Ma with ~ 530 Ma defined by the significantly discordant analyses 1.1, 3.2, and 5.1. There is thus limited evidence for a middle Archean, early igneous crystallization event at ~ 3180 Ma (see also data for sample 85-20H discussed below) with a subsequent metamorphic overprint at ~ 2975 Ma. These Archean cores and rims have been significantly affected by radiogenic Pb loss during the Ross orogeny at ~ 530 Ma.

The metamorphic rim to grain 2 has a prismatic, terminated shape suggesting topotactic growth on an older igneous core (Fig. 3b). Analysis 2.2 is close to concordant with a $^{207}\text{Pb}/^{206}\text{Pb}$ age of ~ 1710 Ma, and indicates the remainder of the complex zircon history for this sample. Together with other rim areas interpreted to be of

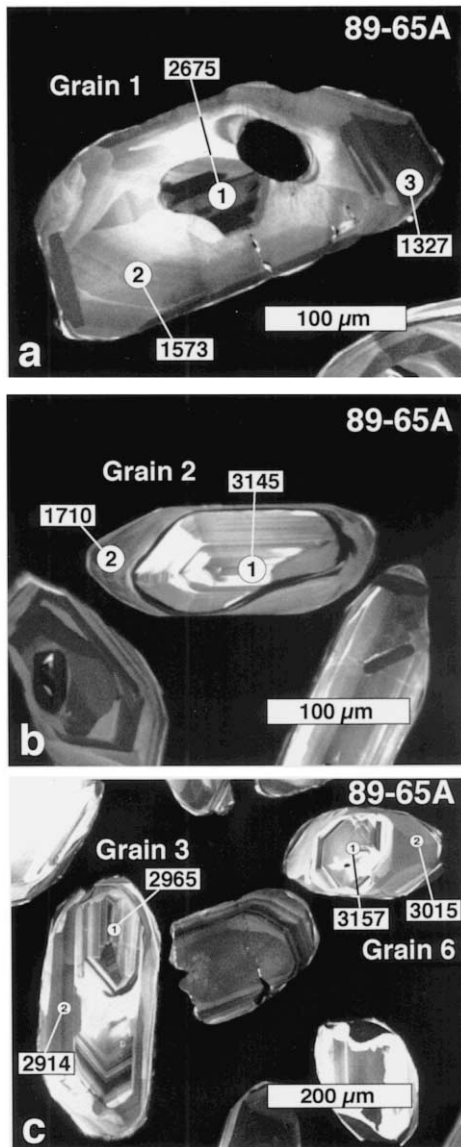


Fig. 3.

Fig. 3. Cathodoluminescence (CL) images of representative zircons from layered gneiss sample 89-65A, showing locations and ages of areas analyzed (labeled as in Table 1). Generally, bright areas have low Th/U ratios and dark areas have higher Th/U (except for grains with $\text{U} = 10^3\text{--}10^4$ ppm, which also appear dark in CL). For each grain, the analysis number is circled and number in the rectangle is interpreted U–Pb age in Ma (generally the $^{207}\text{Pb}/^{206}\text{Pb}$ age for ~ 3000 and ~ 1720 Ma zircons). Data for all zircons are presented in Table 1 and summarized on concordia diagrams in Fig. 4. (a) Grain 1, showing a core with growth banding indicative of igneous crystallization at 2675 Ma, and a complex overgrowth yielding discordant younger ages. Resorption of the remnant core and sector-zoning of the overgrowth suggests new metamorphic growth at about 1700 Ma, followed by Ross-age Pb-loss. (b) Grain 2, showing interior oscillatory growth banding of a euhedral igneous crystal formed at 3145 Ma, truncated by a curved resorption surface, upon which a texturally homogeneous metamorphic overgrowth formed at 1710 Ma. (c) Two grains, 3 and 6, showing internal domains reflecting igneous growth of euhedral crystals at about 3100–3000 Ma, with slightly younger banded or sector-zoned overgrowths indicative of secondary igneous or metamorphic growth 3000–2900 Ma.

Table 1
SHRIMP U–Pb zircon results for layered gneiss sample 89-65A, Nimrod Group, Miller Range, Antarctica

| Grain.spot | U (ppm) | Th (ppm) | Th/U | Pb* (ppm) | ²⁰⁴ Pb/ ²⁰⁶ Pb | f206 (%) | Radiogenic ratios | | | | | | Ages (Ma) | | | | | | Conc. (%) |
|------------|---------|----------|------|-----------|--------------------------------------|----------|---------------------------------------|---------------------------------------|--|---------------------------------------|---------------------------------------|--|---------------------------------------|---------------------------------------|--|----|------|----|-----------|
| | | | | | | | ²⁰⁶ Pb/ ²³⁸ U ± | ²⁰⁷ Pb/ ²³⁵ U ± | ²⁰⁷ Pb/ ²⁰⁶ Pb ± | ²⁰⁶ Pb/ ²³⁸ U ± | ²⁰⁷ Pb/ ²³⁵ U ± | ²⁰⁷ Pb/ ²⁰⁶ Pb ± | ²⁰⁶ Pb/ ²³⁸ U ± | ²⁰⁷ Pb/ ²³⁵ U ± | ²⁰⁷ Pb/ ²⁰⁶ Pb ± | | | | |
| 1.1 | 236 | 51 | 0.21 | 124 | 0.000054 | 0.07 | 0.2535 | 0.0048 | 6.376 | 0.158 | 0.1824 | 0.0025 | 1457 | 25 | 2029 | 22 | 2675 | 23 | 55 |
| 1.2 | 108 | 98 | 0.91 | 51 | 0.000023 | 0.04 | 0.2066 | 0.0033 | 2.772 | 0.057 | 0.0973 | 0.0011 | 1211 | 18 | 1348 | 15 | 1573 | 21 | 77 |
| 1.3 | 278 | 142 | 0.51 | 75 | — | <0.01 | 0.1320 | 0.0022 | 1.556 | 0.032 | 0.0855 | 0.0009 | 799 | 13 | 953 | 13 | 1327 | 19 | 60 |
| 2.1 | 44 | 33 | 0.74 | 56 | 0.000105 | 0.13 | 0.5243 | 0.0124 | 17.63 | 0.459 | 0.2438 | 0.0020 | 2718 | 53 | 2970 | 25 | 3145 | 13 | 86 |
| 2.2 | 216 | 102 | 0.48 | 128 | 0.000043 | 0.07 | 0.2876 | 0.0043 | 4.155 | 0.074 | 0.1048 | 0.0009 | 1630 | 22 | 1665 | 15 | 1710 | 15 | 95 |
| 3.1 | 203 | 117 | 0.58 | 210 | 0.000022 | 0.03 | 0.4542 | 0.0071 | 13.64 | 0.24 | 0.2178 | 0.0014 | 2414 | 31 | 2725 | 17 | 2965 | 10 | 81 |
| 3.2 | 292 | 78 | 0.27 | 278 | 0.000022 | 0.03 | 0.4482 | 0.0059 | 13.05 | 0.19 | 0.2111 | 0.0011 | 2387 | 26 | 2683 | 14 | 2914 | 9 | 82 |
| 4.1 | 65 | 35 | 0.54 | 55 | 0.000127 | 0.16 | 0.3592 | 0.0136 | 11.24 | 0.51 | 0.2270 | 0.0045 | 1979 | 65 | 2544 | 43 | 3031 | 32 | 65 |
| 5.1 | 75 | 44 | 0.58 | 28 | 0.000293 | 0.38 | 0.1675 | 0.0042 | 3.382 | 0.123 | 0.1465 | 0.0034 | 998 | 23 | 1500 | 29 | 2305 | 41 | 43 |
| 5.2 | 138 | 79 | 0.57 | 43 | — | −0.03 | 0.1479 | 0.0031 | 1.766 | 0.056 | 0.0866 | 0.0018 | 889 | 18 | 1033 | 21 | 1352 | 41 | 66 |
| 6.1 | 79 | 63 | 0.80 | 111 | 0.000078 | <0.01 | 0.5755 | 0.0107 | 19.49 | 0.41 | 0.2457 | 0.0019 | 2930 | 44 | 3067 | 20 | 3157 | 12 | 93 |
| 6.2 | 250 | 84 | 0.34 | 312 | — | <0.01 | 0.5726 | 0.0091 | 17.75 | 0.31 | 0.2248 | 0.0013 | 2919 | 37 | 2976 | 17 | 3015 | 9 | 97 |

Uncertainties given at the 1σ level. f206 denotes the percentage of ²⁰⁶Pb that is common Pb. Correction for common Pb made using the measured ²⁰⁶Pb/²⁰⁴Pb ratios. For % conc., 100% denotes a concordant analysis.

metamorphic origin (for example, areas 1.2, 1.3 and 5.2), a third discordia array can be proposed extending from near analysis 2.2 at ~ 1720 Ma to the Ross orogeny overprint and inferred time of radiogenic Pb loss at ~ 530 Ma. Hornblende and muscovite from a similar layered gneiss yielded $^{40}\text{Ar}/^{39}\text{Ar}$ mineral cooling ages between about 525–490 Ma (Goodge and Dallmeyer, 1992, 1996); these Ar ages reflect regional metamorphic temperatures of ~ 500 °C that likely contributed to the recognized Ross-age zircon radiogenic Pb-loss event. We therefore interpret a two-stage, post-Archean metamorphic history for this rock, with significant but distinguishable thermal events at ~ 1720 and ~ 530 Ma.

Zircon CL images and U–Pb data for layered gneiss sample 85-20H were discussed by Goodge and Fanning (1999), but the complete analytical data are presented here (Table 2; 34 individual analyses). Zircons in this gneiss also reveal a multi-stage history beginning with initial ~ 3000

Ma magmatism and metamorphism, followed by ~ 1720 Ma high-grade metamorphism, and ~ 530 Ma metamorphism and partial melting. The age distribution and isotopic behavior of the total zircon population resemble that of sample 89-65A, with inferred simple mixing between multiple age components analyzed from discrete domains. We focus here on the ~ 1720 Ma group (Fig. 5). Zircons of this age are distinguished by dark appearance and textural homogeneity in CL images, with average ratio $\text{Th}/\text{U} = 0.28$. They occur either as cores to prismatic grains or as relatively wide overgrowths on round Archean cores. In most cases, overgrowths cover cores showing rational crystal faces or slightly round external shapes, suggesting topotactic growth on an unmodified or weakly modified igneous core. Whether as cores or overgrowths, the CL images of these domains mostly show an absence of oscillatory zoning, suggesting subsolidus growth during metamorphism.

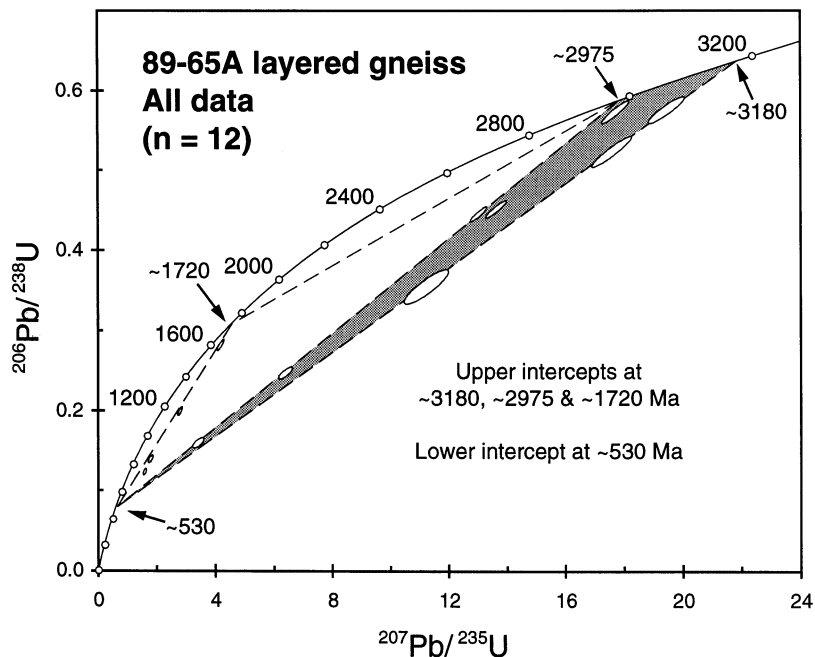


Fig. 4. Concordia diagram of zircon analyses from layered gneiss sample 89-65A (all analyses). Uncertainties are 1σ . Total population distributed on two major arrays: one of highly discordant zircons (in gray shaded area) projecting downward from about 3180–2975 Ma, and the other projecting from about 1720 Ma. Dashed lines show these generalized mixing trends, attributed to Pb-loss events at ~ 1720 and ~ 530 Ma. Age means calculated by data-point errors only.

Table 2
SHRIMP U–Pb zircon results for layered gneiss sample 85-20H, Nimrod Group, Miller Range, Antarctica

| Grain.spot | U (ppm) | Th (ppm) | Th/U | Pb* (ppm) | ²⁰⁴ Pb/ ²⁰⁶ Pb <i>f</i> ₂₀₆ (%) | Radiogenic ratios | | | | | | Ages (Ma) | | | Conc. (%) | | | | |
|------------|---------|----------|-------|-----------|--|---------------------------------------|---------------------------------------|--|---------------------------------------|---------------------------------------|--|-----------|------|-----|-----------|----|------|----|-----|
| | | | | | | ²⁰⁶ Pb/ ²³⁸ U ± | ²⁰⁷ Pb/ ²³⁵ U ± | ²⁰⁷ Pb/ ²⁰⁶ Pb ± | ²⁰⁶ Pb/ ²³⁸ U ± | ²⁰⁷ Pb/ ²³⁵ U ± | ²⁰⁷ Pb/ ²⁰⁶ Pb ± | | | | | | | | |
| 1.1 | 449 | 233 | 0.52 | 367 | 0.000007 | 0.01 | 0.6123 | 0.0069 | 20.27 | 0.24 | 0.2401 | 0.0004 | 3079 | 28 | 3104 | 11 | 3120 | 3 | 99 |
| 1.2 | 9 | <1 | 0.01 | 1 | 0.000838 | 1.52 | 0.0905 | 0.0042 | | | | | 559 | 25 | | | | | |
| 1.3 | 12 | | | 1 | 0.002936 | 5.26 | 0.1098 | 0.0047 | | | | | 672 | 27 | | | | | |
| 2.1 | 188 | 32 | 0.17 | 132 | 0.000024 | 0.03 | 0.5753 | 0.0085 | 17.26 | 0.28 | 0.2175 | 0.0011 | 2930 | 35 | 2949 | 16 | 2963 | 8 | 99 |
| 2.2 | 291 | 80 | 0.28 | 101 | 0.000023 | 0.04 | 0.3005 | 0.0040 | 4.36 | 0.07 | 0.1051 | 0.0007 | 1694 | 20 | 1704 | 13 | 1717 | 12 | 99 |
| 3.1 | 446 | 30 | 0.07 | 303 | 0.000123 | 0.16 | 0.5636 | 0.0072 | 17.47 | 0.24 | 0.2247 | 0.0007 | 2882 | 30 | 2961 | 13 | 3015 | 5 | 96 |
| 3.2 | 431 | 92 | 0.21 | 304 | 0.000015 | 0.02 | 0.5703 | 0.0072 | 17.03 | 0.22 | 0.2165 | 0.0006 | 2909 | 30 | 2936 | 13 | 2955 | 4 | 98 |
| 4.1 | 7 | <1 | <0.01 | 1 | 0.002705 | 1.71 | 0.0856 | 0.0046 | | | | | 529 | 27 | | | | | |
| 5.1 | 174 | 77 | 0.44 | 127 | 0.000030 | 0.04 | 0.5940 | 0.0083 | 18.00 | 0.28 | 0.2197 | 0.0013 | 3006 | 34 | 2990 | 15 | 2979 | 9 | 101 |
| 5.2 | 22 | | | 2 | — | 0.64 | 0.0880 | 0.0029 | | | | | 544 | 17 | | | | | |
| 6.1 | 77 | | | 7 | — | 0.60 | 0.0845 | 0.0015 | | | | | 523 | 9 | | | | | |
| 7.1 | 55 | | | 42 | 0.000012 | 0.02 | 0.5941 | 0.0125 | 18.16 | 0.41 | 0.2217 | 0.0014 | 3006 | 51 | 2998 | 22 | 2993 | 10 | 100 |
| 8.1 | 497 | 98 | 0.20 | 174 | 0.000024 | 0.04 | 0.3117 | 0.0037 | 4.57 | 0.06 | 0.1063 | 0.0004 | 1749 | 18 | 1743 | 11 | 1736 | 6 | 101 |
| 8.2 | 797 | 35 | 0.04 | 71 | 0.000038 | 0.05 | 0.0865 | 0.0010 | | | | | 535 | 6 | | | | | |
| 9.1 | 308 | 36 | 0.12 | 203 | 0.000020 | 0.03 | 0.5468 | 0.0073 | 16.17 | 0.23 | 0.2145 | 0.0006 | 2812 | 30 | 2887 | 13 | 2940 | 5 | 96 |
| 10.1 | 268 | 88 | 0.33 | 93 | 0.000036 | 0.06 | 0.3003 | 0.0038 | 4.32 | 0.06 | 0.1044 | 0.0007 | 1693 | 19 | 1697 | 12 | 1703 | 12 | 99 |
| 10.2 | 312 | 83 | 0.26 | 232 | 0.000010 | 0.01 | 0.5951 | 0.0073 | 17.98 | 0.23 | 0.2191 | 0.0006 | 3010 | 30 | 2988 | 12 | 2974 | 4 | 101 |
| 11.1 | 748 | 93 | 0.12 | 510 | 0.000012 | 0.02 | 0.5599 | 0.0104 | 17.33 | 0.48 | 0.2244 | 0.0041 | 2866 | 43 | 2953 | 27 | 3013 | 29 | 95 |
| 12.1 | 198 | 32 | 0.16 | 64 | 0.000010 | 0.02 | 0.2868 | 0.0037 | 4.52 | 0.07 | 0.1142 | 0.0008 | 1626 | 18 | 1734 | 13 | 1868 | 12 | 87 |
| 13.1 | 192 | 54 | 0.28 | 57 | 0.000050 | 0.08 | 0.2601 | 0.0037 | 3.71 | 0.07 | 0.1033 | 0.0009 | 1490 | 19 | 1573 | 14 | 1685 | 16 | 88 |
| 13.2 | 314 | 52 | 0.17 | 220 | 0.000006 | 0.01 | 0.5675 | 0.0083 | 18.04 | 0.44 | 0.2305 | 0.0041 | 2897 | 34 | 2992 | 24 | 3056 | 29 | 95 |
| 14.1 | 145 | 67 | 0.46 | 52 | — | <0.01 | 0.2995 | 0.0046 | 4.37 | 0.07 | 0.1057 | 0.0007 | 1689 | 23 | 1706 | 14 | 1727 | 11 | 98 |
| 14.2 | 1505 | 52 | 0.03 | 1157 | 0.000002 | 0.00 | 0.6342 | 0.0068 | 21.24 | 0.24 | 0.2429 | 0.0007 | 3166 | 27 | 3150 | 11 | 3139 | 5 | 101 |
| 15.1 | 483 | 161 | 0.33 | 360 | — | <0.01 | 0.5861 | 0.0067 | 17.75 | 0.21 | 0.2196 | 0.0006 | 2974 | 27 | 2976 | 12 | 2978 | 4 | 100 |
| 16.1 | 137 | 44 | 0.32 | 46 | 0.000097 | 0.15 | 0.2880 | 0.0044 | 4.17 | 0.08 | 0.1051 | 0.0011 | 1631 | 22 | 1669 | 16 | 1716 | 19 | 95 |
| 16.2 | 766 | 65.0 | 0.08 | 505 | 0.000012 | 0.02 | 0.5467 | 0.0064 | 16.87 | 0.21 | 0.2238 | 0.0005 | 2812 | 27 | 2928 | 12 | 3009 | 4 | 94 |
| 17.1 | 740 | 33 | 0.04 | 519 | 0.000010 | 0.01 | 0.5897 | 0.0065 | 17.64 | 0.20 | 0.2169 | 0.0005 | 2988 | 26 | 2970 | 11 | 2958 | 4 | 101 |
| 18.1 | 589 | 133 | 0.22 | 340 | 0.000089 | 0.11 | 0.4578 | 0.0070 | 14.58 | 0.24 | 0.2310 | 0.0011 | 2430 | 31 | 2788 | 16 | 3059 | 8 | 79 |
| 19.1 | 246 | 41 | 0.17 | 174 | 0.000010 | 0.01 | 0.5757 | 0.0087 | 17.80 | 0.29 | 0.2243 | 0.0010 | 2931 | 36 | 2979 | 16 | 3012 | 7 | 97 |
| 20.1 | 308 | 46 | 0.15 | 54 | — | <0.01 | 0.1567 | 0.0019 | 1.93 | 0.03 | 0.0895 | 0.0009 | 938 | 10 | 1092 | 11 | 1414 | 19 | 66 |
| 21.1 | 605 | 33 | 0.05 | 53 | 0.000027 | 0.06 | 0.0843 | 0.0011 | | | | | 521 | 6 | | | | | |
| 21.2 | 263 | 58 | 0.22 | 195 | 0.000000 | 0.00 | 0.5968 | 0.0073 | 18.29 | 0.25 | 0.2222 | 0.0010 | 3017 | 29 | 3005 | 13 | 2997 | 7 | 101 |
| 22.1 | 639 | 67 | 0.10 | 193 | 0.000018 | 0.03 | 0.2746 | 0.0030 | 3.99 | 0.05 | 0.1053 | 0.0004 | 1564 | 15 | 1631 | 10 | 1719 | 8 | 91 |
| 22.2 | 420 | 59 | 0.14 | 266 | 0.000004 | 0.01 | 0.5224 | 0.0333 | 15.33 | 1.03 | 0.2129 | 0.0029 | 2709 | 143 | 2836 | 66 | 2927 | 22 | 93 |

Uncertainties given at the 1σ level. *f*₂₀₆ denotes the percentage of ²⁰⁶Pb that is common Pb. For areas >800 Ma, correction for common Pb made using the measured ²⁰⁴Pb/²⁰⁶Pb ratio. For areas <800 Ma, correction for common Pb made using the measured ²³⁸U/²⁰⁶Pb and ²⁰⁷Pb/²⁰⁶Pb following Tera and Wasserburg (1972) as outlined in Compston et al. (1992).

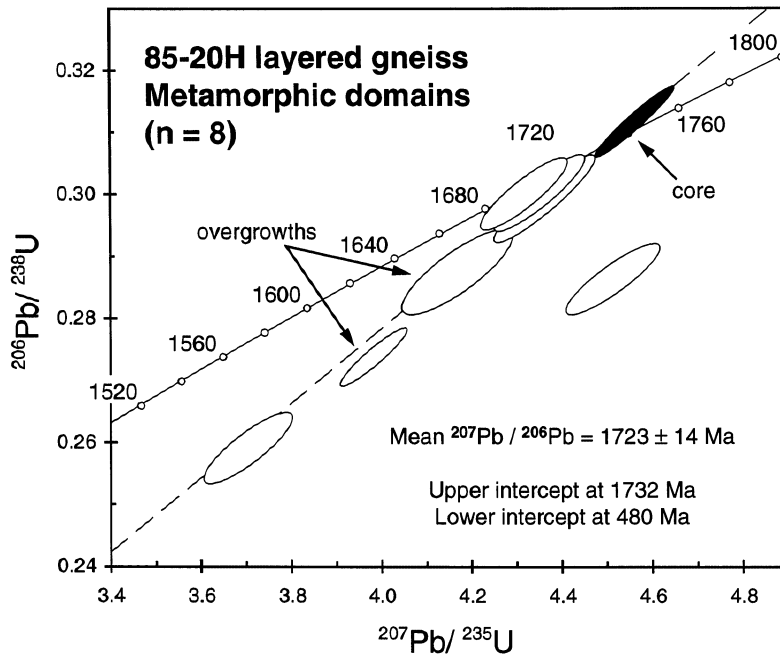


Fig. 5. Concordia diagram of zircon analyses yielding ages of about 1730 Ma from layered gneiss sample 85-20H (from Goode and Fanning (1999)). Uncertainties are 1σ . Analyses include zircon cores (black) and overgrowths (unfilled). The core of grain 8 yielded a concordant $^{207}\text{Pb}/^{206}\text{Pb}$ age of 1736 ± 6 Ma (Table 2). This sample also contains texturally distinct zircon domains yielding igneous and/or metamorphic crystallization ages of about 3100–3000 and 530 Ma (Goode and Fanning, 1999), similar to the distribution of ages in sample 89-65 presented here (Fig. 4).

Analyses of seven domains of this type in 85-20H yielded a weighted mean $^{207}\text{Pb}/^{206}\text{Pb}$ age of 1723 ± 14 Ma with slight excess scatter (MSWD = 2.4) mainly arising from inferred radiogenic Pb loss during a Ross-age event. Inclusion of the extremely discordant analysis 20.1 to a pooled regression gives an upper intercept at 1732 ± 22 Ma and a lower intercept at 480 ± 110 Ma with MSWD = 2.1 (Fig. 5). Forcing a regression through ~ 530 Ma (MSWD = 1.9) yielded an older (~ 1740 Ma) upper intercept. Six of the seven domains are wide overgrowths on Archean cores showing prismatic external terminations; one analysis is from a prismatic core (grain 8.1) yielding a $^{207}\text{Pb}/^{206}\text{Pb}$ age of 1736 ± 6 Ma. Based on the pooled regression and the age from analysis 8.1, we interpret ~ 1730 Ma as the best estimate for the age of Paleoproterozoic metamorphism in this sample. Goode and Fanning (1999) interpreted these zircon domains as the result of new subsolidus growth, rather than

anatexis or metamorphic recrystallization, because of a lack of igneous growth features, low Th/U ratios, occurrence as both core and overgrowth, and general concordance at an age that cannot be produced by simple isotopic disequilibrium between ~ 3000 and ~ 500 Ma events. Therefore, the ~ 1730 Ma zircon domains in this gneiss, like those in sample 89-65A, may reflect high-temperature metamorphism that is contemporaneous with spatially associated magmatic events (see below).

3.2. Eclogites

Numerous mafic and ultramafic tectonic blocks occur within the Nimrod Group, particularly along the boundaries of pelitic schist and quartzfeldspathic gneiss (Fig. 1; Goode et al. 1993a; Peacock and Goode, 1995). The ellipsoidal mafic and ultramafic blocks range in size from 0.5 to 50 meters in diameter. Mafic blocks are the more

common of the two; in some cases they appear to be detached from a continuous layer that experienced boudinage during Ross deformation. The origin of the block protoliths is discussed below, but they probably represent metamorphosed mafic intrusions such as basaltic or diabasic dikes and sills. Tectonite foliation in the host schists and gneisses wraps around the blocks (Fig. 2c), and foliation within the blocks, where present, is generally discordant to foliation in the enclosing schists and gneisses. Some blocks contain curved dilational veins of plagioclase + quartz which taper toward the margin with host gneisses; where asymptotic to the block margin, these veins show a vorticity that is compatible with the sense of shear recorded by fabrics in enclosing ductile tectonites (Peacock and Goodge, 1995).

Most of the mafic tectonic blocks have dark amphibolitic rinds consisting of hornblende + plagioclase \pm biotite \pm garnet, whereas dark-green cores of the blocks consist of massive, fine-grained relict eclogite mineral assemblages. Presently, the cores contain pyrope-rich garnet + clinopyroxene symplectite + hornblende + plagioclase + quartz

+ ilmenite \pm orthopyroxene \pm biotite. The symplectites were interpreted by Peacock and Goodge (1995) as recrystallization textures formed from jadeitic clinopyroxene during decompression. The mineral assemblages and compositions, amphibolite rinds, and symplectite intergrowths indicate that these mafic blocks represent partially re-equilibrated eclogites. Discordant block and host foliations, and sigmoidal block-cutting veins, show that they acted as semi-rigid bodies within the ductile Nimrod tectonites during amphibolite-facies Ross deformation.

Sample 90-131A is a partially retrogressed eclogite from the core of a mafic tectonic block enclosed by layered gneisses near Gerard Bluffs (Fig. 1; location 83°35'23" S; 157°10' E). This phacoidal block is approximately 3 m in size, and contains an outer 5–30 cm rim of black, coarse-grained amphibolite. The core is dark-green in color, massive and fine-grained. Our sample from the core zone contains small (0.25–0.50 mm) equant grains of garnet (about 35–40 modal per cent) surrounded by symplectite intergrowths of clinopyroxene, plagioclase, Ca-amphibole, and an

opaque mineral (Fig. 2d). In samples from similar blocks, garnets contain 13–22 mol% pyrope (Peacock and Goodge, 1995), falling within the Group C eclogite field of Coleman et al. (1965). Quartz occurs in irregular pockets (= 0.5 mm) surrounded by symplectite intergrowths; it is spatially isolated from garnet and is not part of the symplectite assemblage, suggesting it formed from excess Si produced during symplectite formation. Petrographic and mineralogical data from similar blocks are discussed in detail by Peacock and Goodge (1995). We studied additional samples from the eclogite suite, including a mafic block (90-130D) from the same outcrop area as sample 90-131A that contains garnet and symplectite with a similar textural relation. Detailed back-scattered electron imaging and electron microprobe analysis show that garnets in sample 90-130D contain minute inclusions of omphacitic pyroxene (Table 3). The omphacite inclusions are Ca–Na pyroxene (Morimoto et al., 1988) with Na/(Na + Ca) = 0.35–0.40, similar to omphacite in eclogitic rocks from many high-grade gneiss terrains. The inclusions contain about 32 mol% jadeite and minimal acmite components; both compositions are generally similar to analyses of the symplectite replacement assemblage obtained by broad-beam analysis (compare inclusions from 90-130D with symplectite intergrowths in ANT-54H, Table 3), although the omphacites are notably richer in Al and Na. Given that plagioclase is not a stable phase under eclogite-facies conditions, and that relict garnet is presently surrounded by rims of plagioclase, it is possible that these elements migrated from areas of omphacite breakdown during retrogressive symplectite formation, leading to crystallization of albite along the pyroxene-garnet boundaries and yielding low Al and Na in the residual symplectites.

This is the first report of omphacite in the Nimrod Group, confirming earlier conclusions based on mineralogical evidence that these mafic blocks indeed represent relict eclogites. Together, the presence of omphacite in sample 90-130D and the occurrence of garnet-symplectite textures in many mafic blocks suggest that eclogite-facies metamorphism was pervasive in the Nimrod Group, even if not presently preserved in the host

gneisses. We believe the mineralogical relations in 90-130D and other samples described by Peacock and Goodge (1995) are representative of sample 90-131A because of their textural and mineralogical similarity.

Table 3
Representative analyses of omphacitic pyroxene inclusions in garnet from eclogite blocks

| Sample | 90-130D, Inc. 2 | 90-130D, Inc. 3 | ANT-54H ^a |
|--------------------------------|--------------------|--------------------|----------------------|
| SiO ₂ | 52.46 | 52.60 | 51.79 |
| TiO ₂ | 0.27 | 0.32 | 0.15 |
| Al ₂ O ₃ | 8.74 | 8.47 | 5.50 |
| Cr ₂ O ₃ | 0.00 | 0.02 | 0.02 |
| FeO ^T | 9.62 | 9.37 | 12.74 |
| MnO | 0.06 | 0.02 | 0.08 |
| MgO | 8.06 | 8.24 | 9.84 |
| CaO | 14.67 | 14.23 | 16.39 |
| Na ₂ O | 4.39 | 5.03 | 1.72 |
| K ₂ O | — | — | 0.09 |
| Total | 98.27 | 98.30 | 98.32 |
| Si | 1.956 | 1.949 | 1.977 |
| Al (iv) | 0.044 | 0.051 | 0.023 |
| Al (vi) | 0.340 | 0.318 | 0.224 |
| Ti | 0.008 | 0.009 | 0.004 |
| Cr | 0.000 | 0.001 | 0.001 |
| Fe ³⁺ | 0.007 | 0.076 | 0.000 |
| Fe ²⁺ | 0.293 | 0.214 | 0.407 |
| Mn | 0.002 | 0.001 | 0.003 |
| Mg | 0.448 | 0.455 | 0.560 |
| Ca | 0.586 | 0.565 | 0.670 |
| Na | 0.317 | 0.361 | 0.127 |
| K | — | — | 0.004 |
| Σ Cations | 4.000 | 4.000 | 4.000 |
| Mg/(Mg+Fe ²⁺) | 0.60 | 0.68 | 0.58 |
| Na/(Na+Ca) | 0.35 | 0.39 | 0.16 |
| Jd% | 31.7 | 32.1 | |
| Ac% | 0.0 | 4.3 | |
| Ca.FeTs% | 0.4 | 0.0 | |
| Ca.TiTs% | 0.8 | 0.9 | |
| Ca.Ts% | 2.6 | 1.7 | |
| Woll% | 27.5 | 27.2 | |
| En% | 22.4 | 22.9 | |
| Fs% | 14.7 | 10.8 | |

Pyroxenes normalized to 6 oxygens; endmember proportions following Morimoto et al. (1988) and Cawthorn and Collerson (1974) for mineral analyses only.

^a Broad-beam electron microprobe analysis of clinopyroxene intergrowths in symplectite (from Peacock and Goodge (1995)).

Peacock and Goodge (1995) suggested that formation of the eclogitic parageneses preceded Ross events, but lacking direct age constraints were unable to determine whether (a) the eclogites formed independently during a separate metamorphic stage and were later entrained by the host gneisses during Ross deformation, or (b) the eclogites formed during an early high-*P* phase of Ross activity. To test these possibilities, we recovered zircon from eclogite sample 90-131A. The abundant zircons in this sample are uniformly about 100 μm in diameter, multi-faceted crystals with equant spherical forms (classic ‘soccer-ball’ shape as seen in many eclogites) and interior sector zoning (Fig. 6). Zoning patterns include pie-wedge sectors radiating from the centers of grains (e.g. grain 2, Fig. 6a) and concentric growth sectors (e.g. grain 14, Fig. 6b). These morphological and textural features are common for zircon that has crystallized under high-*P* metamorphic conditions (Paquette et al., 1989; Gebauer and Grunfelder, 1979; Rubatto et al., 1999). Many of the grains in sample 90-131A have a very thin (= 10 μm) outer rim that is distinctly bright in CL; it is similar to low-Th rims in other Nimrod Group samples that yielded Ross crystallization ages of about 540–520 Ma (Goodge and Fanning, 1999).

Twenty-seven areas were analyzed on 22 grains (Table 4). The Th/U ratios are mostly in the range 0.25–0.40, normal for igneous zircons. The U and Th contents are moderate to low (U mostly in the range 50–150 ppm and Th 15–80 ppm), but they are not indicative of a particular paragenesis. The general morphology of the zircons, ‘soccer ball’ or multi-faceted round shape coupled with the internal sector zonation highlighted in the CL images, suggests deep-crustal metamorphic crystallization, yet their chemistry is more consistent with a crustal, magmatic origin. One possible explanation is that the zircon crystallized initially from a gabbroic melt, and that the superimposed deep-crustal metamorphic recrystallization was essentially isochemical in the absence of a fractionated fluid.

On a Wetherill concordia plot the analyses form a somewhat dispersed, quasi-concordant

Table 4
SHRIMP U–Pb zircon results for eclogite sample 90-131A, Nimrod Group, Miller Range, Antarctica

| Grain spot | U (ppm) | Th (ppm) | Th/U | Pb* (ppm) | $^{204}\text{Pb}/^{206}\text{Pb}$ | f206 (%) | Radiogenic ratios | | | | | Ages (in Ma) | | | | | Conc. (%) | | |
|------------|---------|----------|------|-----------|-----------------------------------|----------|--------------------------------------|--------------------------------------|---------------------------------------|--------------------------------------|--------------------------------------|--------------------------------------|------|----|------|----|-----------|----|-----|
| | | | | | | | $^{206}\text{Pb}/^{238}\text{U} \pm$ | $^{207}\text{Pb}/^{235}\text{U} \pm$ | $^{207}\text{Pb}/^{206}\text{Pb} \pm$ | $^{206}\text{Pb}/^{238}\text{U} \pm$ | $^{207}\text{Pb}/^{235}\text{U} \pm$ | $^{207}\text{Pb}/^{206}\text{U} \pm$ | | | | | | | |
| 1.1 | 322 | 117 | 0.36 | 107 | 0.000037 | 0.06 | 0.2833 | 0.0021 | 4.028 | 0.041 | 0.1031 | 0.0007 | 1608 | 10 | 1640 | 8 | 1681 | 12 | 96 |
| 1.2 | 87 | 26 | 0.30 | 22 | 0.000046 | 0.07 | 0.2162 | 0.0034 | 2.922 | 0.056 | 0.0980 | 0.0009 | 1262 | 18 | 1388 | 15 | 1587 | 18 | 80 |
| 2.1 | 111 | 30 | 0.27 | 38 | 0.000059 | 0.09 | 0.2994 | 0.0030 | 4.344 | 0.072 | 0.1053 | 0.0013 | 1688 | 15 | 1702 | 14 | 1719 | 22 | 98 |
| 3.1 | 138 | 50 | 0.36 | 47 | – | <0.01 | 0.2895 | 0.0029 | 4.203 | 0.055 | 0.1053 | 0.0008 | 1639 | 15 | 1675 | 11 | 1720 | 13 | 95 |
| 3.2 | 101 | 29 | 0.29 | 62 | 0.000033 | 0.05 | 0.3076 | 0.0058 | 4.4787 | 0.109 | 0.106 | 0.0014 | 1729 | 29 | 1727 | 20 | 1725 | 24 | 100 |
| 4.1 | 166 | 53 | 0.32 | 52 | 0.000063 | 0.10 | 0.2709 | 0.0024 | 3.812 | 0.050 | 0.1021 | 0.0009 | 1545 | 12 | 1595 | 11 | 1662 | 16 | 93 |
| 5.1 | 40 | 16 | 0.39 | 13 | – | 0.49 | 0.2799 | 0.0058 | 4.116 | 0.105 | 0.1066 | 0.0014 | 1591 | 29 | 1657 | 21 | 1743 | 24 | 91 |
| 6.1 | 77 | 25 | 0.33 | 21 | 0.000310 | 0.02 | 0.2322 | 0.0030 | 3.178 | 0.091 | 0.0993 | 0.0024 | 1346 | 16 | 1452 | 22 | 1610 | 45 | 84 |
| 7.1 | 56 | 20 | 0.37 | 19 | 0.000010 | 0.08 | 0.2936 | 0.0055 | 4.260 | 0.105 | 0.1052 | 0.0015 | 1660 | 27 | 1686 | 20 | 1718 | 26 | 97 |
| 8.1 | 129 | 36 | 0.28 | 37 | 0.000050 | 0.60 | 0.2527 | 0.0033 | 3.566 | 0.059 | 0.1024 | 0.0009 | 1452 | 17 | 1542 | 13 | 1667 | 16 | 87 |
| 9.1 | 42 | 12 | 0.28 | 14 | 0.000383 | 0.15 | 0.2864 | 0.0084 | 3.913 | 0.166 | 0.0991 | 0.0027 | 1624 | 42 | 1616 | 35 | 1607 | 52 | 101 |
| 10.1 | 135 | 66 | 0.49 | 46 | 0.000098 | 0.13 | 0.2838 | 0.0051 | 4.083 | 0.093 | 0.1044 | 0.0013 | 1610 | 26 | 1651 | 19 | 1703 | 22 | 95 |
| 11.1 | 171 | 48 | 0.28 | 50 | 0.000080 | 0.07 | 0.2521 | 0.0053 | 3.596 | 0.088 | 0.1035 | 0.0011 | 1449 | 27 | 1549 | 20 | 1687 | 20 | 86 |
| 12.1 | 201 | 75 | 0.38 | 60 | 0.000041 | 0.07 | 0.2496 | 0.0060 | 3.730 | 0.117 | 0.1084 | 0.0019 | 1437 | 31 | 1578 | 25 | 1772 | 32 | 81 |
| 12.1b | 162 | 57 | 0.35 | 52 | 0.000043 | 0.07 | 0.2763 | 0.0042 | 4.032 | 0.081 | 0.1058 | 0.0012 | 1573 | 21 | 1641 | 16 | 1729 | 21 | 91 |
| 12.2 | 211 | 71 | 0.34 | 133 | 0.000038 | 0.06 | 0.2952 | 0.0018 | 4.288 | 0.040 | 0.1054 | 0.0007 | 1667 | 9 | 1691 | 8 | 1721 | 12 | 97 |
| 13.1 | 78 | 22 | 0.28 | 75 | 0.000039 | 0.06 | 0.3063 | 0.0025 | 4.422 | 0.057 | 0.1047 | 0.0009 | 1722 | 12 | 1717 | 11 | 1709 | 16 | 101 |
| 14.1 | 149 | 57 | 0.38 | 27 | 0.000083 | 0.13 | 0.2971 | 0.0049 | 4.289 | 0.090 | 0.1047 | 0.0011 | 1677 | 25 | 1691 | 17 | 1709 | 20 | 98 |
| 14.2 | 378 | 159 | 0.42 | 51 | 0.00019 | 0.03 | 0.2918 | 0.0028 | 4.183 | 0.057 | 0.1040 | 0.0009 | 1650 | 14 | 1671 | 11 | 1696 | 16 | 97 |
| 15.1 | 46 | 14 | 0.30 | 28 | 0.000498 | 0.78 | 0.3122 | 0.0083 | 4.4381 | 0.170 | 0.103 | 0.0025 | 1751 | 41 | 1720 | 32 | 1681 | 46 | 104 |
| 16.1 | 47 | 17 | 0.36 | 27 | 0.000175 | 0.28 | 0.2908 | 0.0066 | 4.1365 | 0.127 | 0.103 | 0.0019 | 1646 | 33 | 1662 | 25 | 1682 | 34 | 98 |
| 17.1 | 76 | 20 | 0.27 | 40 | 0.000058 | 0.09 | 0.2711 | 0.0056 | 3.7071 | 0.102 | 0.099 | 0.0016 | 1546 | 28 | 1573 | 22 | 1609 | 30 | 96 |
| 18.1 | 73 | 20 | 0.28 | 43 | 0.000026 | 0.04 | 0.3033 | 0.0062 | 4.3469 | 0.111 | 0.104 | 0.0013 | 1708 | 31 | 1702 | 21 | 0696 | 24 | 101 |
| 19.1 | 83 | 22 | 0.26 | 42 | 0.000246 | 0.39 | 0.2616 | 0.0050 | 3.6099 | 0.114 | 0.100 | 0.0023 | 1498 | 25 | 1552 | 26 | 0626 | 44 | 92 |
| 20.1 | 35 | 11 | 0.31 | 21 | – | <0.01 | 0.3025 | 0.0110 | 4.6407 | 0.217 | 0.111 | 0.0028 | 1704 | 55 | 1757 | 40 | 1820 | 47 | 94 |
| 21.1 | 82 | 25 | 0.30 | 50 | 0.000085 | 0.13 | 0.3058 | 0.0062 | 4.4523 | 0.113 | 0.106 | 0.0014 | 1720 | 31 | 1722 | 21 | 1725 | 24 | 100 |
| 22.1 | 71 | 22 | 0.31 | 43 | 0.000085 | 0.13 | 0.3029 | 0.0060 | 4.3864 | 0.120 | 0.105 | 0.0017 | 1706 | 30 | 1710 | 23 | | 31 | 100 |

Uncertainties given at the 1σ level. f206 denotes the percentage of ^{206}Pb that is common Pb. Correction for common Pb made using the measured $^{206}\text{Pb}/^{204}\text{Pb}$ ratios. For % conc., 100% denotes a concordant analysis.

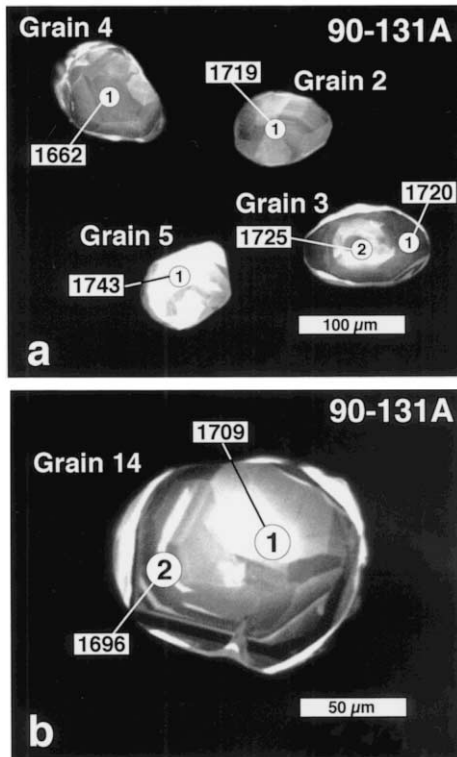


Fig. 6. Cathodoluminescence (CL) images of representative zircons from eclogite sample 90-131A, showing locations and ages of areas analyzed (labeled as in Table 4). (a) Four grains, 2–5, showing typical small, round, equant forms and interior sector zoning. These features are all common in zircon crystallized at high-*P* metamorphic conditions (Krogh et al., 1974; Peucat et al., 1982; Paquette et al., 1989). All grains yield approximately 1700 Ma ages, although grain 4 appears notably younger than the rest. (b) Grain 14, showing internal structure of eclogite zircons in detail. Two analyses yielded highly concordant ages of about 1700 Ma; although the core analysis yielded a slightly older age, the $^{207}\text{Pb}/^{206}\text{Pb}$ ages are statistically indistinguishable. This grain, like many others in the sample, contains a very thin ($= 10 \mu\text{m}$) rim that is distinctly bright in CL; it is similar to low-Th rims in other Nimrod Group samples that yielded Ross crystallization ages of about 540–520 Ma (see Goodge and Fanning (1999)).

cluster, although some radiogenic Pb loss is evident (Fig. 7). The 21 most concordant analyses yielded a weighted mean $^{207}\text{Pb}/^{206}\text{Pb}$ age of 1704 ± 11 Ma. However, as many of the analyses are more than 5% discordant, it is more meaningful to fit a discordia regression line to all 27 analyses. The regression has slight excess scatter

(MSWD = 1.7) with an upper concordia intercept at 1723 ± 29 Ma and a lower intercept at ~ 510 Ma with a large uncertainty. Grains that have more than one internal domain in CL (e.g. grains 3 and 14, Fig. 6) show no substantial difference in their ages. The data show no evidence of older Proterozoic or Archean igneous components, reflecting either complete zircon recrystallization under high-grade metamorphic conditions or that no zircon existed in the rock prior to ~ 1720 Ma.

Overall, these data reflect zircon growth during recrystallization of Nimrod Group mafic protoliths under eclogite-facies conditions at ~ 1720 Ma. They represent, therefore, some of the oldest dated eclogitic rocks (see Gebauer, 1990; Messiga et al., 1990). The zircons show evidence of radiogenic Pb loss during Ross thermomechanical events, reflected geologically by structural dismemberment of the eclogite-facies rocks into discrete blocks, retrogression of the block rims, and replacement of jadeitic clinopyroxene by symplectite. Based on these new ages, the variety of mineralogical features in the eclogitic blocks discussed by Peacock and Goodge (1995) can be seen to be petrogenetically distinct from younger Ross features.

3.3. Orthogneiss

The Nimrod Group includes a variety of metagneous rocks, ranging from megacrystic granodiorite to equigranular felsite, leucogranite, diorite, aplite, and pegmatite, often associated with migmatites. Many of these units occur as thin, sheet-like bodies interlayered with gneiss or schist units on a scale of several centimeters to tens of meters, and they display ductile tectonite fabrics of variable intensity (Goodge et al., 1993a). Several individual units have yielded U–Pb zircon ages of 540–520 Ma (Goodge et al., 1993b), representing syn-kinematic emplacement and, locally, anatexis within the Nimrod basement during high-*T* Ross orogenesis. As such, generation of these units immediately preceded the emplacement of late-stage, post-tectonic granite plutons belonging to the Granite Harbour suite (Fig. 1).

One of the prominent metaigneous units in the Nimrod Group is a compositionally homogeneous body of granodiorite orthogneiss exposed in the Camp Ridge area that contains distinctive augen-shaped K-feldspar megacrysts. Earlier workers interpreted the elongate K-feldspar ‘lenticles’ as the product of feldspathization of a sedimentary protolith during high-grade metamorphism and associated K-metasomatism (see Grindley et al., 1964; Gunner, 1969, 1983). Field relations and petrographic textures of the augen gneiss unit indicate that it is a mylonitic orthogneiss formed by the ductile deformation of a plutonic, rather than a sedimentary, protolith (Goodge et al., 1991, 1993a). Primary contact relations among Nimrod rock units are obscured by strong ductile deformation, but this orthogneiss was observed to intrude schist at one locality. Thus, the coarse-grained, augen-shaped K-feldspar porphyroclasts are relict igneous phenocrysts altered in shape by ductile strain, rather than by metaso-

matic infiltration. This orthogneiss unit was previously termed the Aurora Formation (Grindley et al., 1964), but has subsequently been referred to as Camp Ridge granodiorite (Borg et al., 1990) and Camp Ridge orthogneiss (Goodge et al., 1993a) to reflect its igneous rather than sedimentary origin. It is important to note that there are several petrographically and texturally similar orthogneiss units in the Nimrod Group, including one with a U–Pb zircon age of 540 Ma (90-WMR-4 from Goodge et al. (1993b)).

Sample M-28 comes from the Camp Ridge orthogneiss in the western Miller Range (Fig. 1; location 83°11′06″ S; 155°52′ E). Here the unit displays variably intense L–S tectonite fabrics, grading locally to dark bands of ultramylonite. Textural shear-sense indicators, including asymmetrical S–C fabrics and rotated K-feldspar δ -porphyroclasts, are common and kinematically compatible with other tectonites from the Nimrod Group. Sample M-28 contains quartz, microcline,

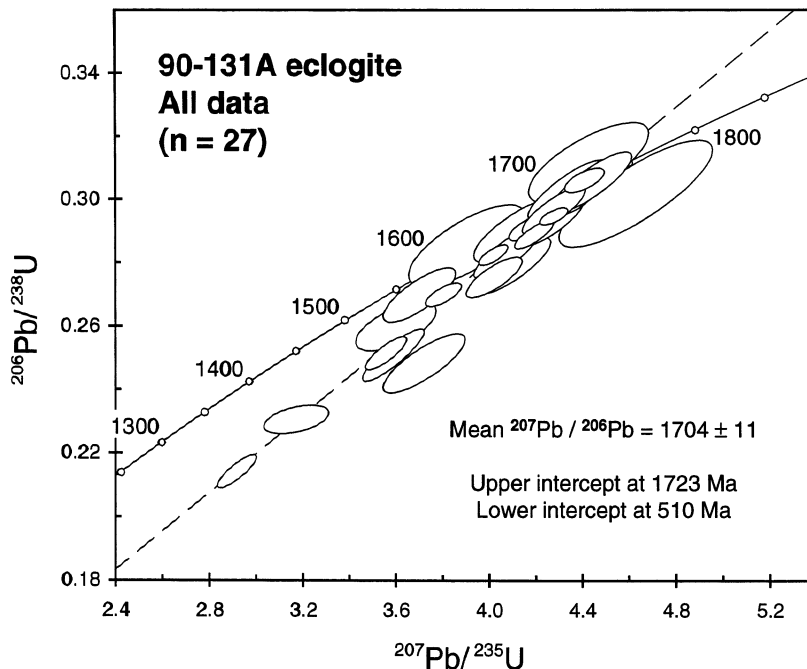


Fig. 7. Concordia diagram of zircon analyses from eclogite sample 90-131A (all analyses). Most grains analyzed are concordant to within 10% (see Table 4), yielding a weighted mean $^{207}\text{Pb}/^{206}\text{Pb}$ age of about 1704 ± 11 Ma. Fitting a discordia (dashed line) to all data yields an upper intercept age of 1723 ± 29 Ma, which we interpret as the best estimate for the age of eclogite-facies recrystallization. Distribution along the array is attributed to Pb-loss at about 530 Ma.

plagioclase, biotite, hornblende, and accessory epidote, apatite, sphene, zircon and Fe-oxide. It is medium grained and well foliated with anastomosing, weakly defined S–C asymmetry (Fig. 2b). Feldspars, including the coarse microcline megacrysts, contain deformation bands, bent twins, and microfaults, reflecting both crystal-plastic and brittle intracrystalline strain. Quartz shows undulose extinction with minor subgrain formation and local ribbon texture.

Because there are abundant metaigneous units in the Nimrod Group that give Ross crystallization ages, the age of this mylonitic orthogneiss unit is of critical importance in helping to constrain Ross and older events. Goodge et al. (1991) referred to preliminary U–Pb data measured by isotope-dilution techniques indicating a $^{207}\text{Pb}/^{206}\text{Pb}$ crystallization age of ~ 1.7 Ga for sample M-28. This age was important in establishing a minimum age limit for other Nimrod metasedimentary units, and it provided a maximum age limit of ~ 1700 Ma for Nimrod Group metamorphism and ductile deformation. Subsequent SHRIMP analyses, first briefly reported by Bennett and Fanning (1993), are presented here.

Most of the grains in M-28 are simple zoned magmatic zircon, showing oscillatory-zoned structure across the grain or within wide outer domains (Fig. 8). Grains such as 13 and 14 have CL-dark, mottled cores with round outline that we have not analyzed. The dark cores of these grains probably represent inherited xenocrystic(?) material, in accord with the elevated Nd initial ratio for this orthogneiss unit (Borg et al., 1990). The zircons have moderate U and Th contents, and relatively uniform Th/U ratios averaging 0.73 (Table 5). Analysis of the zoned magmatic exteriors from 14 grains yielded essentially concordant data (all but one are concordant to within 10%) with a weighted mean $^{207}\text{Pb}/^{206}\text{Pb}$ age of 1730 ± 14 Ma (Fig. 9). The dark central area of grain 10 yielded a similar age to the zoned outer components of other grains and is interpreted to be part of a single magmatic crystallization event for this grain. As with other Nimrod samples, the slight discordance of some grains in M-28 is attributed to minor radiogenic Pb-loss during Ross-age metamorphic and igneous events. Hornblende

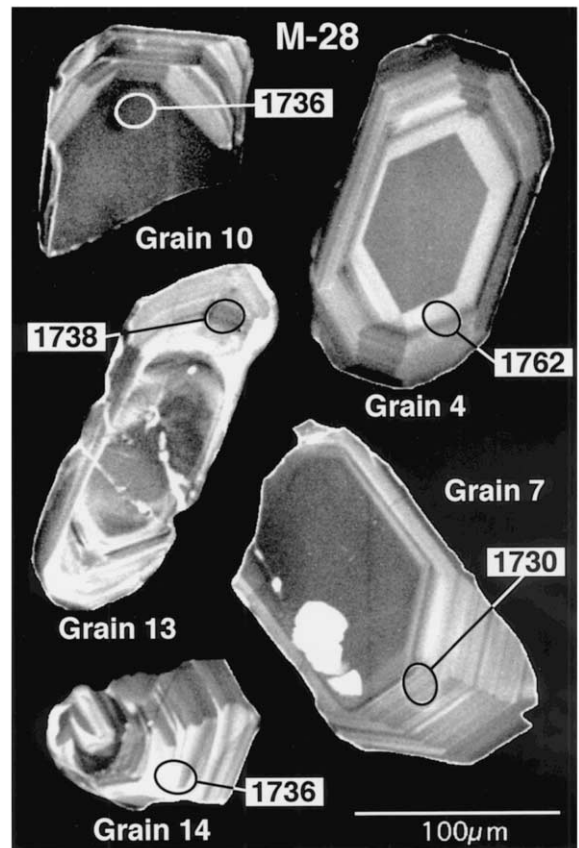


Fig. 8. Cathodoluminescence (CL) images of representative zircons analyzed from orthogneiss sample M-28, showing locations and ages of areas analyzed (labeled as in Table 5). Most grains are simple zoned magmatic zircon, showing oscillatory-zoned outer domains yielding concordant ages within error of the weighted-mean age (Table 5). Grains 13 and 14 have mottled, elongate cores with round outline that we have not analyzed. The central domains to these grains may represent inherited older material, in accord with the elevated Nd initial ratio for this orthogneiss unit (Borg et al., 1990).

from a different sample of the same orthogneiss unit yielded a $^{40}\text{Ar}/^{39}\text{Ar}$ plateau cooling age of 509.3 ± 1.4 Ma, and an isotope correlation age of 506.7 ± 2.1 Ma (Goodge and Dallmeyer, 1992), reflecting metamorphic temperatures of ≈ 500 °C that are consistent with a Ross-age zircon Pb-loss event. We interpret the ~ 1730 Ma weighted mean zircon age as the time of igneous crystallization of the orthogneiss, based on zircon morphology, their moderate U and Th contents, their high

Table 5
SHRIMP U–Pb zircon results for orthogneiss sample M-28, Nimrod Group, Miller Range, Antarctica

| Grain.spot | U (ppm) | Th (ppm) | Th/U | Pb* (ppm) | ²⁰⁴ Pb/ ²⁰⁶ Pb <i>f</i> ₂₀₆ (%) | Radiogenic ratios | | | | | | Ages (Ma) | | | | | | Conc. (%) | |
|------------|---------|----------|------|-----------|--|---------------------------------------|---------------------------------------|--|---------------------------------------|---------------------------------------|--|-----------|------|-----|------|----|------|-----------|-----|
| | | | | | | ²⁰⁶ Pb/ ²³⁸ U ± | ²⁰⁷ Pb/ ²³⁵ U ± | ²⁰⁷ Pb/ ²⁰⁶ Pb ± | ²⁰⁶ Pb/ ²³⁸ U ± | ²⁰⁷ Pb/ ²³⁵ U ± | ²⁰⁷ Pb/ ²⁰⁶ Pb ± | | | | | | | | |
| 1.1 | 187 | 159 | 0.85 | 66 | 0.000174 | 0.27 | 0.3014 | 0.0081 | 4.296 | 0.153 | 0.1034 | 0.0021 | 1698 | 40 | 1693 | 30 | 1686 | 38 | 101 |
| 2.1 | 140 | 83 | 0.60 | 49 | 0.000010 | 0.02 | 0.3157 | 0.0097 | 4.573 | 0.157 | 0.1051 | 0.0013 | 1769 | 48 | 1744 | 29 | 1715 | 22 | 103 |
| 3.1 | 309 | 205 | 0.66 | 108 | 0.000023 | 0.04 | 0.3127 | 0.0090 | 4.530 | 0.139 | 0.1051 | 0.0008 | 1754 | 44 | 1736 | 26 | 1715 | 14 | 102 |
| 4.1 | 155 | 96 | 0.62 | 52 | 0.000023 | 0.04 | 0.3014 | 0.0091 | 4.478 | 0.166 | 0.1078 | 0.0020 | 1698 | 45 | 1727 | 31 | 1762 | 34 | 96 |
| 5.1 | 102 | 66 | 0.65 | 31 | 0.000010 | 0.02 | 0.2731 | 0.0107 | 4.026 | 0.175 | 0.1069 | 0.0016 | 1556 | 54 | 1639 | 36 | 1748 | 27 | 89 |
| 6.1 | 147 | 125 | 0.85 | 56 | — | <0.01 | 0.3249 | 0.0100 | 4.847 | 0.197 | 0.1082 | 0.0025 | 1814 | 49 | 1793 | 35 | 1769 | 42 | 103 |
| 7.1 | 168 | 104 | 0.62 | 56 | 0.000197 | 0.31 | 0.2976 | 0.0089 | 4.346 | 0.158 | 0.1059 | 0.0018 | 1679 | 44 | 1702 | 31 | 1730 | 32 | 97 |
| 8.1 | 213 | 195 | 0.92 | 78 | 0.000024 | 0.04 | 0.3086 | 0.0238 | 4.516 | 0.405 | 0.1061 | 0.0039 | 1734 | 118 | 1734 | 77 | 1734 | 69 | 100 |
| 9.1 | 219 | 209 | 0.95 | 72 | — | <0.01 | 0.2744 | 0.0075 | 4.043 | 0.128 | 0.1068 | 0.0014 | 1563 | 38 | 1643 | 26 | 1746 | 24 | 90 |
| 10.1 | 157 | 100 | 0.64 | 49 | 0.000018 | 0.03 | 0.2788 | 0.0102 | 4.083 | 0.164 | 0.1062 | 0.0013 | 1585 | 52 | 1651 | 33 | 1736 | 22 | 91 |
| 11.1 | 242 | 138 | 0.57 | 77 | — | <0.01 | 0.2865 | 0.0089 | 4.276 | 0.169 | 0.1082 | 0.0023 | 1624 | 45 | 1689 | 33 | 1770 | 39 | 92 |
| 12.1 | 220 | 152 | 0.69 | 74 | 0.000145 | 0.23 | 0.2998 | 0.0082 | 4.327 | 0.143 | 0.1047 | 0.0016 | 1690 | 41 | 1699 | 28 | 1709 | 29 | 99 |
| 13.1 | 346 | 331 | 0.96 | 129 | — | <0.01 | 0.3113 | 0.0116 | 4.565 | 0.204 | 0.1064 | 0.0022 | 1747 | 57 | 1743 | 38 | 1738 | 38 | 101 |
| 14.1 | 153 | 98 | 0.64 | 49 | — | <0.01 | 0.2869 | 0.0082 | 4.204 | 0.153 | 0.1063 | 0.0021 | 1626 | 41 | 1675 | 30 | 1736 | 36 | 94 |

Uncertainties given at the 1σ level. *f*₂₀₆ denotes the percentage of ²⁰⁶Pb that is common Pb. Correction for common Pb made using the measured ²⁰⁶Pb/²⁰⁴Pb ratios. For % conc., 100% denotes a concordant analysis.

Th/U ratios, and the uniform ages obtained from all the zircon areas analyzed. Therefore, the 1730 Ma age for this orthogneiss documents the production of felsic magmas during Paleoproterozoic time. Only the oscillatory-zoned outer domains were analyzed in order to precisely determine a crystallization age for this unit. Measured $\epsilon_{\text{Nd}}(0)$ of -26 and a depleted-mantle Nd-model age of 2.73 Ga (Borg et al., 1990) for another split of the original sample suggest that the igneous protolith was derived from older crustal sources or assimilated older crustal components. This event may have melted a crustal source similar to other gneiss and schist units in the Nimrod Group with depleted-mantle Nd-model ages of 2.7–3.1 Ga (Borg et al., 1990; Borg and DePaolo, 1994). Partial crustal assimilation is consistent with the presence of some mottled zircon cores that show round outlines suggesting a xenocrystic origin (Fig. 8), although no analyses were performed.

4. Discussion

4.1. Nature of the Nimrod Orogeny

The new U–Pb zircon data from the Nimrod Group indicate a major period of deep-crustal metamorphism and magmatism at ~ 1730 – 1720 Ma. Zircons from two samples of layered gneiss with Archean igneous precursors show metamorphic overgrowths of ~ 1730 – 1720 Ma, and an eclogite block preserved within the gneisses contains zircons with a similar metamorphic crystallization age. A deformed granodioritic plutonic body that intrudes gneisses and metasedimentary rocks yielded a concordant zircon crystallization age of ~ 1730 Ma. The SHRIMP age data from these petrologically different samples indicate that Nimrod crust was intruded by plutons at ~ 1730 Ma, and that high- T and high- P metamorphic recrystallization occurred by at least ~ 1730 Ma, culminating in high- P parageneses at ~ 1720 Ma.

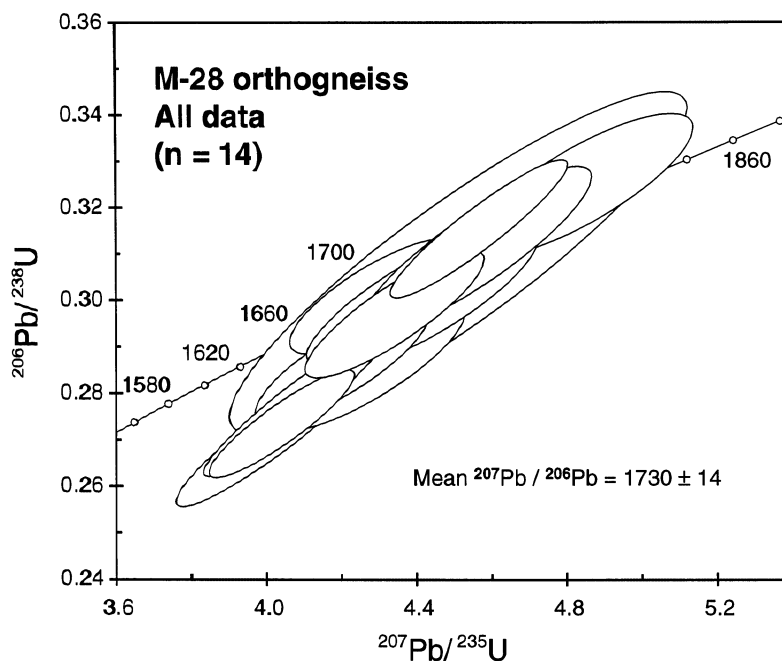


Fig. 9. Concordia diagram of zircon analyses from orthogneiss sample M-28 (all analyses). Essentially concordant data yielded a weighted mean $^{207}\text{Pb}/^{206}\text{Pb}$ age of 1730 ± 14 Ma. Age means calculated by data-point errors only.

Together, these data reveal an important period of orogenic activity between about 1730–1720 Ma, and they may constrain the true age of the Nimrod Orogeny as originally conceived by Grindley and Laird (1969). They defined the Nimrod Orogeny to describe the unique high-grade petrologic and structural features in crystalline basement rocks of the Nimrod Group that are not observed in adjacent low-grade supracrustal units. Although correct in distinguishing the high-grade metamorphic imprint, Grindley and Laird (1969) based the Precambrian age for the Nimrod Orogeny on K–Ar mineral ages that were later shown to be invalid because of extraneous Ar components (Adams et al., 1982; Goodge and Dallmeyer, 1992). Furthermore, the characteristic metamorphic and deformation features in the Nimrod Group are now known to be a consequence of Ross-age orogenic processes (Goodge and Dallmeyer, 1992, 1996; Goodge et al., 1993b). We therefore recommend association of the term Nimrod Orogeny with the Paleoproterozoic igneous and metamorphic events described here.

Because field and structural relations are poorly preserved, we are unable to characterize the structural geometry and tectonic relationships of the Nimrod Orogeny in detail. However, from the age and petrologic relations described above, it is possible to outline a general interpretation of Paleoproterozoic events (Fig. 10). Basement of the East Antarctic shield, as represented by the Nimrod Group, consisted primarily of layered metasedimentary and metaigneous gneisses prior to about 1700 Ma. Geochronological evidence from the layered gneiss samples discussed here, as well as in earlier studies (Bennett and Fanning, 1993; Goodge and Fanning, 1999), suggests that ~3100 Ma crust in this part of the shield was formed by largely magmatic processes and thermally stabilized by ~3000–2950 Ma, with possible anatexis modification at ~2500 Ma. It is possible that the Nimrod protoliths consisted of unmetamorphosed sedimentary and volcanic materials just prior to ~1730 Ma, but this is less likely given evidence for earlier Archean metamorphism. At some time before 1730 Ma, the gneisses were intruded by mafic dikes and/or sills, represented by mafic layers and boudins in the present gneissic assemblage. During

the ~1730–1720 Ma Nimrod Orogeny (Fig. 10a), this crustal assemblage was reactivated by metamorphism to eclogite- and high-*P* granulite-facies conditions, and intruded by granodioritic magmas. The association of high-*P* metamorphism and magmatism reflects mid- to lower-crustal conditions for the Nimrod Orogeny. Crustal rocks in this deep part of the orogen probably experienced thermal restabilization well before the next major orogenic phase at ~500 Ma, but we have no direct evidence to document the timing or rate of equilibration.

Evidence for deep-seated metamorphism comes solely from metamorphic zircon overgrowths in the layered gneisses and new metamorphic zircon growth during eclogite formation. There is no preservation of high-grade pre-Ross metamorphic mineral assemblages in the layered gneisses that can be differentiated from the Ross parageneses with certainty. However, the zircon textures are consistent with high-grade metamorphic growth at 1730–1720 Ma. Eclogite parageneses are partially preserved only in mafic blocks within the layered gneiss assemblage (Peacock and Goodge, 1995), likely because of inhibited back-reaction kinetics. New zircons in these eclogite bodies with the multi-faceted, equant appearance that is characteristic of zircon crystallized under high-*P* indicate that eclogite recrystallization occurred at ~1720 Ma. Although the ages of metamorphism in the layered gneisses and eclogites overlap within error, a younger age of eclogite crystallization may indicate more sluggish reactions compared to the gneisses, possibly due to nucleation kinetics and low volatile content. Petrologic data presented by Peacock and Goodge (1995) indicate equilibration of eclogites at 12–25 kbar, or 40–90 km depth. In general, the metamorphic parageneses are quite similar to occurrences in the Scandinavian Caledonides (e.g. Mysen and Heier, 1972; Bryhni et al., 1977; Griffin et al., 1985; Cuthbert and Carswell, 1990), and may represent in situ eclogitization of lower crust. The high pressures attending metamorphism and eclogite formation in diverse rock types and the high temperatures associated with coeval magma emplacement suggest that the Nimrod Orogeny involved crustal thickening brought about by plate convergence and/or collision.

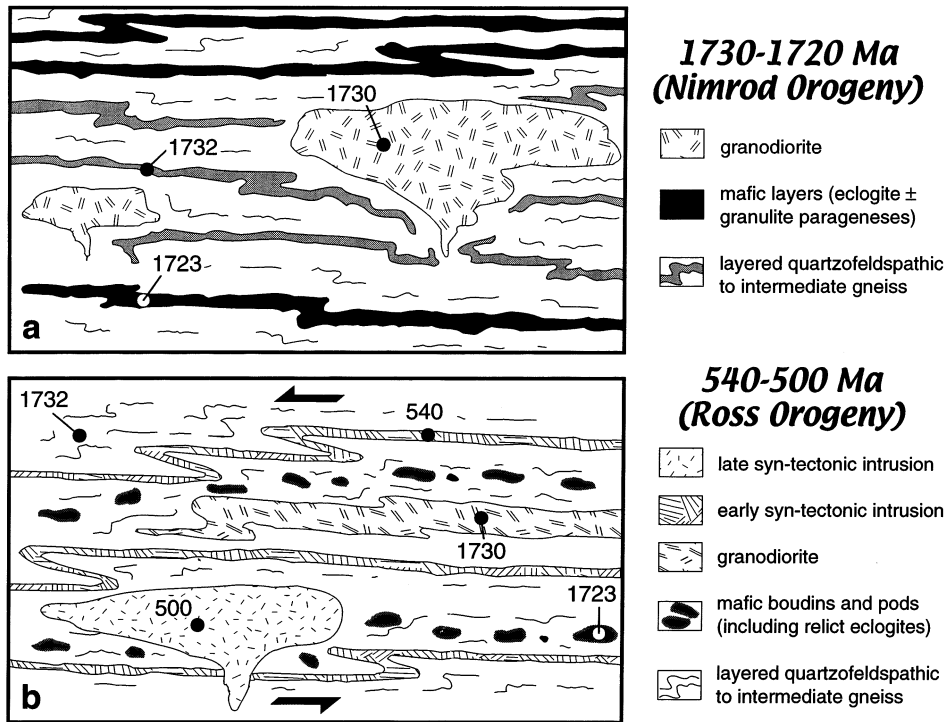


Fig. 10. Diagram summarizing geologic and age relationships within the Nimrod Group during the ~1700 Ma Nimrod Orogeny and younger Ross events. (a) Nimrod Group during the 1730–1720 Ma Nimrod Orogeny, reflecting lower-crustal high-*P* metamorphism and magmatism. Protoliths of the gneissic units are ~3100–2950 Ma igneous rocks representing juvenile magmatic crust of the East Antarctic shield (Goodge and Fanning, 1999). Primary age of mafic units, possibly originated as igneous dikes, is unknown. Metamorphic conditions at this stage are difficult to assess because of strong Ross-age overprinting, but high-*P* and high-*T* granulite and eclogite facies metamorphism are inferred at ~1700 Ma from relict phase relations and SHRIMP zircon ages in the gneisses and eclogite bodies reported here. Layered gneisses were intruded at this time by the ~1730 Ma Camp Ridge granodiorite, and possibly by other undated units. (b) Effects of the Ross Orogeny at 540–500 Ma, including penetrative ductile shear, shown by arrows, and emplacement of syn- and late-kinematic intrusive sheets and plutons. During Ross time, the Nimrod basement was strongly mechanically reactivated (Goodge et al., 1993a), producing a consistent set of top-SE structures, deformation and upper-amphibolite facies metamorphism in all units, and boudinage of the eclogitic mafic layers, yielding relict eclogitic cores preserved in individual blocks. Ongoing magmatism resulted in the emplacement of syn-tectonic (~540–520 Ma) to late tectonic (~515–500 Ma) intrusions.

If our interpretation of ~1730 Ma orogenic thickening is correct, it provides a likely mechanism to explain detrital zircon ages obtained from Nimrod Group quartzites, which yielded ages spanning 2555–1734 Ma (Walker and Goodge, 1991). The quartzites are presently in structural contact with layered gneisses within the 12 km thick Ross-age Miller Range shear zone (Goodge et al., 1993a), but they reflect deposition of sandstone after ~1700 Ma. It is possible that these quartzites reflect a sedimentary response to orogenic activity by uplift of igneous and/or meta-

morphic basement during the time of the Nimrod Orogeny; as such, there may be an ‘older’ gneiss package that is geologically and stratigraphically distinct from the ‘younger’ metasedimentary assemblage within the composite Nimrod Group. If so, there may be an important but cryptic suture or overlap boundary within the Nimrod Group, although it has been intensely modified by Ross-age ductile strain.

Rocks of the Nimrod Group show the effects of active-margin Ross orogenesis on crystalline basement of the East Antarctic shield. These effects

are shown in Fig. 10b, including formation of new high-strain ductile shear fabrics in metamorphic and igneous precursors, transposition and obliteration of pre-existing structures, and boudinage of stronger mafic eclogitic layers into discrete round blocks (Goodge et al., 1993a). The Ross overprint occurred at high temperatures and high $P(\text{H}_2\text{O})$, such that the only preservation of earlier parageneses is within the cores of eclogitic bodies, which resisted retrogressive re-equilibration due to a combination of kinetic effects and the inability of fluids to permeate the mafic units. Syn- to post-tectonic granitic intrusions also invaded the Nimrod basement during Ross time, and anatexis occurred locally during the formation of migmatitic gneiss. The U–Pb zircon overgrowth ages described here from samples of layered gneiss provide direct evidence for the age of the Ross overprint (~ 530 Ma). This age agrees well with conventional U–Pb zircon dating of syn- to post-tectonic intrusions (540–520 Ma), U–Pb dating of metamorphic monazite (~ 520 Ma), and $^{40}\text{Ar}/^{39}\text{Ar}$ cooling ages of fabric-forming minerals (525–490 Ma) (Goodge and Dallmeyer, 1992, 1996; Goodge et al., 1993b). With a strong petrologic and structural Ross overprinting, the Paleoproterozoic Nimrod orogenesis is evident only from the U–Pb ages obtained for discrete zircon domains by ion microprobe analysis of gneiss, eclogite, and granodiorite. Although all but the orthogneiss were affected by the high- P granulite- to eclogite-facies Nimrod metamorphism, only the relict mafic boudins preserve eclogite-facies assemblages because the other units experienced penetrative deformation and retrogressive metamorphism under upper amphibolite-facies Ross conditions.

4.2. Comparison with other areas

Proterozoic orogenic events during the period 2000–1600 Ma are recognized in many cratonic areas worldwide. In some cases these events appear related to the collision of older cratonic shields, and in other cases they reflect juvenile crustal growth along a cratonic margin. Unique in this regard is a cratonic province encompassing half of the greater East Antarctic shield, part of

southeastern Australia, and the southwestern corner of Laurentia, characterized by Archean to Paleoproterozoic rocks overprinted by a brief and somewhat diachronous orogenic event centered on ~ 1700 Ma. Areas affected by the ~ 1700 Ma events, shown in Fig. 11, include the following: (a) Bunger Hills and Denman Glacier areas of East Antarctica (Black et al., 1992; Sheraton et al., 1992, 1993); (b) Windmill Islands, on the Wilkes Land coast of Antarctica (Williams et al., 1983); (c) Commonwealth Bay and adjacent areas of Terre Adélie Land in Antarctica (Tingey, 1991; Peucat et al., 1999); (d) Eyre Peninsula and Gawler Craton in South Australia (Oliver et al., 1983; Webb et al., 1986; Sheraton et al., 1989; Daly et al., 1998); (e) south of the Yilgarn craton in the Albany–Fraser Orogen of Western Australia (Nelson et al., 1995); (f) Mojave province of the southwestern United States (Wooden and Miller, 1990; Flodin et al., 1997; Barth et al., 2000). Among these, rocks in the Bunger Hills area, Terre Adélie Land, the Gawler Craton, and Mojave province yield chronologies that are strikingly similar to that of the Nimrod Group, as discussed below.

In the Bunger Hills, felsic orthogneisses with U–Pb zircon ages of about 1700–1500 Ma suggest emplacement of Paleoproterozoic to Mesoproterozoic plutons into older Archean gneisses (Sheraton et al., 1993). Here, tonalitic orthogneiss with a 2641 Ma crystallization age represents Archean basement into which 1699 Ma granodiorites were emplaced (Sheraton et al., 1992). Paleoproterozoic igneous rocks in the nearby western Denman Glacier area give 3.59–1.60 Ga depleted-mantle Nd model ages, suggesting partial melting of discrete Archean and Paleoproterozoic crustal components at ~ 1700 –1600 Ma to yield a range of model ages from isotopic mixing (Black et al., 1992). Together these data suggest that Archean crust in the Bunger Hills was modified by ~ 1700 Ma metamorphism and intracrustal melting. In Terre Adélie Land, Rb–Sr metamorphic ages of 1650–1300 Ma suggest mid- to Late Proterozoic reworking of pre-existing crust (Tingey 1991), but this history is refined considerably with more recent U–Pb zircon age data (Peucat et al., 1999). These authors report U–Pb ages of 1720 Ma and

older from zircon cores in migmatitic basement, succeeded by ~ 1690 Ma zircon rims and metamorphic monazite of the same age. The metamorphic patterns and ages from this gneissic terrain suggest sedimentary deposition of the migmatite precursors between 1720 and 1690 Ma, followed by high- T /low- P metamorphism at ~ 1690 Ma. Peucat et al. (1999) interpret the metamorphic assemblages and cooling patterns to reflect crustal melting and slow cooling as a result of mafic magmatic underplating associated with litho-

spheric thinning, but heating by crustal thickening is also plausible. Low-grade phyllitic metamorphic rocks from Cape Hunter in Terre Adélie contain detrital zircons with ages between 2500–1700 Ma (Oliver and Fanning, 1997); a dominant population of ~ 1770 Ma places a maximum age limit on deposition, and it indicates that igneous and metamorphic basement of that age was exposed as a source. The similarity with detrital zircons in some Nimrod Group quartzites suggests that a broad region of ~ 1700 Ma crust was

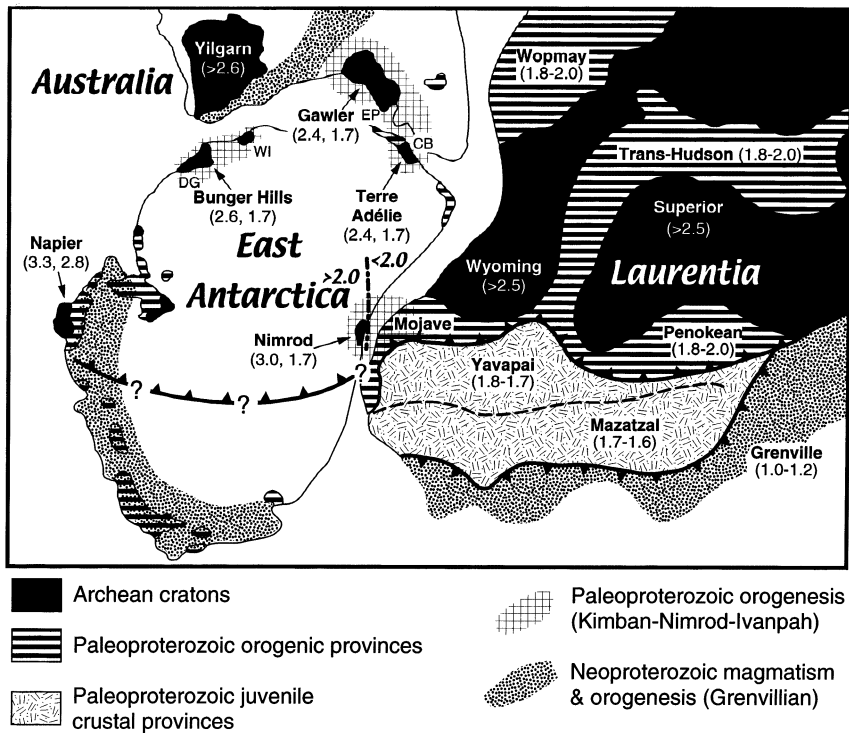


Fig. 11. Map showing reconstruction of major cratonic elements in part of Rodinia supercontinent (after Hoffman, 1991; Moores, 1991; Borg and DePaolo, 1994), also showing distribution of ~ 1700 Ma magmatic and thermal events in the East Antarctic shield, Gawler Craton of Australia, and western Laurentia (hachured). CB Commonwealth Bay; EP Eyre Peninsula; DG Denman Glacier; WI Windmill Islands. Sources of information are cited in the text. Note some reconstructions place Laurentia more directly adjacent to Australia (e.g. Burrett and Berry, 2000). Nimrod Group represents Archean crust of the East Antarctic shield that is overprinted by Paleoproterozoic Nimrod Orogeny. Correlative ~ 1700 Ma events are known from the Bunger Hills (Black et al., 1992; Sheraton et al., 1992, 1993), Gawler craton (Oliver et al., 1983; Fanning et al., 1988; Sheraton et al., 1989; Oliver and Fanning, 1997; Daly et al., 1998), Terre Adélie (Peucat et al., 1999), and the Mojave province of western Laurentia (Wooden and Miller, 1990; Flodin et al., 1997; Barth et al., 2000). Petrologic relations suggest that ~ 1700 Ma events in Terre Adélie are largely the result of thermal-magmatic processes, whereas the Nimrod Group shows petrologic evidence of deep-seated metamorphism related to crustal thickening. We speculate that crustal thickening associated with Nimrod Orogeny may be linked to a collisional event at the outer edge of the greater Antarctic–Laurentian Archean cratonic core. Shown here is a proposed suture extending across East Antarctica that may correlate with the boundary between Paleoproterozoic and Archean provinces in Laurentia (e.g., contractional boundary between the Wyoming and Yavapai–Mazatzal provinces).

exposed due to unroofing following a major igneous and metamorphic orogenic event.

The Gawler craton underlies much of central South Australia and comprises Archean to Mesoproterozoic rocks that have remained substantially undeformed since 1450 Ma (Parker, 1993). As summarized by Daly et al. (1998), the Gawler craton records several metamorphic and igneous events of ~ 1700 Ma age, including: (a) eruption of bimodal volcanics at ~ 1740 Ma (McGregor Volcanics and Moonta porphyry), (b) intrusion of the Middlecamp granite at ~ 1730 Ma, (c) intrusion of Moody Suite granites and other unnamed aplitic intrusions of the Lincoln Complex at ~ 1710 Ma, (d) emplacement of the slightly younger Engenina Granite at ~ 1690 Ma, and (e) granulite-facies metamorphism at ~ 1735 Ma. These magmatic and metamorphic events are recognized primarily in the Eyre Peninsula, but extend northward to the Mount Woods inlier. They are associated in several areas with multi-phase deformation attributed to the Kimban Orogeny, including isoclinal folding and mylonitic shear zone displacement under upper amphibolite- to granulite-facies conditions. South of the Yilgarn craton in Western Australia, orthogneisses in the Biranup Complex of the Albany–Fraser Orogen yield ages of 1634 Ma to 1695 Ma (Nelson et al., 1995), indicating a somewhat younger period of granitic magmatism.

As suggested by several authors (e.g. Sheraton et al., 1993; Oliver and Fanning, 1997), the ~ 1700 Ma igneous and metamorphic events summarized here provide a means of correlating parts of the East Antarctic shield with rocks affected by the Kimban Orogeny in southern Australia. In particular, Oliver and Fanning (1997) noted unique patterns in metamorphism, aeromagnetic signature, and detrital zircon population in metapelites from Commonwealth Bay in Terre Adélie and the southern Eyre Peninsula. The present-day southern margin of Australia, including the Gawler craton, is therefore considered by most workers to have rifted from the Wilkes Land margin of Antarctica in the Cretaceous (Cande and Mutter, 1982; Parker, 1993). On the basis of similar ~ 1700 Ma metamorphic and magmatic histories in basement rocks exposed in Terre Adé-

lie Land and the Eyre Peninsula, Fanning et al. (1995, 1996) suggested these events were part of a common craton-forming stage prior to Rodinia amalgamation. They proposed that this broad juvenile craton, the so-called 'Mawson Continent', extended from southeastern Australia into the Wilkes Land region of East Antarctica (Fig. 11). It is unknown where this basement province extends beyond the narrow coastal exposures of Terre Adélie Land. However, recently compiled aeromagnetic data (Damaske, 1990; Finn et al., 1998) extending across northern Victoria Land in Antarctica suggest that much of the Wilkes Land ice sheet covers crust with a magnetic signature similar to that of the Paleoproterozoic Gawler craton in South Australia. In general terms, then, these correlated magmatic and deep-crustal metamorphic events may reflect an important period of crustal consolidation, similar to that proposed here for ~ 1700 Ma events in the Nimrod Group.

Paleoproterozoic and Mesoproterozoic igneous and metamorphic crust comprises a substantial part of southwestern Laurentia between the southern margin of composite Archean provinces and the Neoproterozoic Grenville orogen (Fig. 11). A substantial part of this Proterozoic crustal material is juvenile and represents the growth and accretion of arc-related volcanic and volcanoclastic materials (Bowring and Karlstrom, 1990; Van Schmus et al., 1993). In the extreme southwestern corner of Laurentia, however, rocks with Paleoproterozoic isotopic signatures suggest the presence of strongly modified older crust (Bennett and DePaolo, 1987). This so-called Mojave province is characterized by a high-grade metamorphic assemblage of sedimentary, volcanic, and plutonic precursors that is intruded by a series of granitoids ranging from ~ 1780 Ma to ~ 1640 Ma age (Wooden and Miller, 1990; Barth et al., 2000). Magmatism was concomitant with granulite-facies metamorphism and migmatization referred to as the Ivanpah Orogeny and dated at ~ 1705 Ma. Igneous rocks in the Mojave province reveal an important Paleoproterozoic magmatic history, including a suite of calc-alkaline orthogneisses with U–Pb zircon ages of 1783–1708 Ma, and a distinctive suite of transitional calc-alkaline to tholeiitic meta-granites with ages of 1690–1640 Ma

(Flodin et al., 1997; Barth et al., 2000). Those authors interpret the older suite as an early calc-alkaline expression of craton-margin subduction, and the younger suite as a consequence of crustal thickening and intracrustal melting. These magmatic relations suggest a similar history as recorded in the previously discussed areas, namely early active-margin processes associated with plate convergence, followed by latest Paleoproterozoic crustal thickening that may be a result of collision between cratonic fragments during amalgamation of supercontinental lithosphere.

4.3. Implications for Proterozoic plate reconstructions

Our new age data from the Nimrod Group, when considered in the context of Paleoproterozoic age relations in the areas noted above, have potentially important tectonic implications for cratonic interactions resulting in supercontinent amalgamation. Although Paleoproterozoic crustal events have been known for some time in the East Antarctic shield, southern Australia, and southwestern Laurentia, the new Nimrod Group ages provide a means to unify these now fragmented areas (Fig. 11). First, evidence for ~1700 Ma metamorphism and magmatism in the Nimrod Group expands considerably the extent of known Paleoproterozoic orogenesis across the greater East Antarctic shield and adjacent Gawler craton of South Australia. These findings suggest that much of the Wilkes Land ice cap between Terre Adélie and the central Transantarctic Mountains is underlain by crust with a major age component of ~1700 Ma. The Nimrod Group is therefore geographically important because it extends our knowledge of Archean and Paleoproterozoic events to the Ross Sea side of the East Antarctic shield.

Second, similarities between the Nimrod Group and rocks of the Mojave province in Laurentia may provide a unique point of geological correlation between East Antarctica and Laurentia. Since initial suggestion of a Neoproterozoic supercontinent comprised in part by East Antarctica, Australia, and Laurentia (Dalziel, 1991; Hoffman, 1991; Moores, 1991), many alternative fits have

been proposed on the basis of geological and paleomagnetic lines of evidence. Some of these (e.g. Ross et al., 1992; Borg and DePaolo, 1994) have used known basement geology to infer a position of Laurentia relative to the East Antarctic–Australian margin prior to breakup at ~750 Ma. Given that rocks with a ~1700 Ma history are an important element on all three modern continents, events of this age may help to constrain supercontinent reconstructions. In Fig. 11 we show a fit between these continents that places the Mojave province adjacent to the present position of the Nimrod Group within the East Antarctic shield. Other proposed reconstructions place Laurentia directly adjacent to modern Australia (e.g. Ross et al., 1992; Brookfield, 1993; Burrett and Berry, 2000), although the geological correlations used for these geometries are not unique. In Fig. 11, we wish to highlight the similarities in cratonic geologic histories as shown by the arrangement of Archean, Paleoproterozoic, and Neoproterozoic provinces. As such, our fit is not uniquely constrained by an alignment of rocks showing a ~1700 Ma history, but it emphasizes the correspondence of *older* parent rocks (3.0–2.0 Ga) that have been modified significantly by 1700 Ma events. We speculatively show a proposed extension into East Antarctica of the Archean–Proterozoic province boundary that is well documented in Laurentia (Wyoming–Yavapai boundary). The Nimrod Group, with its history of Archean crust generation overprinted by younger Paleoproterozoic events, has broad similarities to this fundamental Laurentian boundary. This and other models can be tested with additional geochronology in exposed areas and subsurface geophysics in areas presently covered by ice or surficial deposits.

Finally, the record of deep-crustal metamorphism and magmatism now attributed to the Nimrod Orogeny may reflect a collisional suture between Paleoproterozoic and Archean crustal elements as part of incipient supercontinent assembly. Although many authors link the growth of Rodinia proper to Grenville-age (1200–1000 Ma) events, these are restricted to the outermost margin of present-day East Antarctica and are not known from the Transantarctic Mountains mar-

gin or the Mojave province of southwestern Laurentia. It is possible, therefore, that ~1700 Ma orogenesis represents initial assembly of a proto-Rodinian supercontinent by the consolidation of cratonic elements in present-day East Antarctica, southern Australia, and southwestern Laurentia.

5. Conclusions

New ion microprobe U–Pb zircon age data from metamorphic and metagneous rocks of the Nimrod Group in Antarctica indicate a major period of deep-crustal metamorphism and magmatism at about 1730–1720 Ma. Zircons from Archean layered gneisses show metamorphic overgrowths of ~1730–1720 Ma on older Archean cores, and an eclogitic block preserved within these gneisses contains new metamorphic zircons yielding a metamorphic crystallization age of ~1720 Ma. A deformed granodiorite plutonic body that intrudes gneisses and metasedimentary rocks yielded a concordant zircon crystallization age of ~1730 Ma. Although only scant petrologic evidence is preserved for these metamorphic and igneous events, the zircon age data from diverse rock types indicate they occurred under mid- to deep-crustal conditions, possibly associated with crustal thickening due to cratonic collision. Because prior ages cited in support of a Neoproterozoic (~1000 Ma) Nimrod Orogeny have been shown to be geologically unreliable, we recommend associating the term Nimrod Orogeny instead with the Paleoproterozoic (~1730–1720 Ma) events described here. The Nimrod Orogeny thus correlates well with other tectonic events in East Antarctica, South Australia and southwestern Laurentia that may have played a role in early supercontinent assembly. In particular, early orogenesis in the Nimrod Group may reflect crustal amalgamation during incipient Paleoproterozoic formation of Rodinia.

Acknowledgements

This work was supported by the Office of Polar Programs at the U.S. National Science Founda-

tion (grant OPP-9219818) and by the Research School of Earth Sciences at The Australian National University. We thank two anonymous reviewers for careful review, including numerous comments that helped to clarify our discussion.

References

- Adams, C.J.D., Gabites, J.E., Wodzicki, A., Laird, M.G., Bradshaw, J.D., 1982. Potassium–argon geochronology of the Precambrian–Cambrian Wilson and Robertson Bay Groups and Bowers Supergroup, northern Victoria Land, Antarctica. In: Craddock, C. (Ed.), *Antarctic Geoscience*. University of Wisconsin Press, Madison, WI, pp. 543–548.
- Barth, A.P., Wooden, J.L., Coleman, D.S., Fanning, C.M., 2000. Geochronology of the Proterozoic basement of southwesternmost North America, and the origin and evolution of the Mojave crustal province. *Tectonics* 19, 616–629.
- Bennett, V.C., DePaolo, D.J., 1987. Proterozoic crustal history of the western United States as determined by neodymium isotopic mapping. *Geol. Soc. of Am. Bull.* 99, 674–685.
- Bennett, V.C., Fanning, C.M., 1993. A glimpse of the cryptic Gondwana shield: Archean and Proterozoic ages from the central Transantarctic Mountains. *Geological Society of America Abstracts with Programs* 25, 49.
- Black, L.P., Sheraton, J.W., Tingey, R.J., McCulloch, M.T., 1992. New U–Pb zircon ages from the Denman Glacier area, East Antarctica, and their significance for Gondwana reconstruction. *Antarct. Sci.* 4, 447–460.
- Borg, S.G., DePaolo, D.J., 1994. Laurentia, Australia, and Antarctica as a Late Proterozoic supercontinent: constraints from isotopic mapping. *Geology* 22, 307–310.
- Borg, S.G., DePaolo, D.J., Smith, B.M., 1990. Isotopic structure and tectonics of the central Transantarctic Mountains. *J. of Geophys. Res.* 95, 6647–6669.
- Bowring, S.A., Karlstrom, K.E., 1990. Growth, stabilization, and reactivation of Proterozoic lithosphere in the southwestern United States. *Geology* 18, 1203–1206.
- Brookfield, M.E., 1993. Neoproterozoic Laurentia–Australia fit. *Geology* 21, 683–686.
- Bryhni, I., Krogh, E., Griffin, W.L., 1977. Crustal derivation of Norwegian eclogites: a review. *Neues Jahrbuch für Mineralogie Abhandlungen* 130, 49–68.
- Burrett, C., Berry, R., 2000. Proterozoic Australia–Western United States (AUSWUS) fit between Laurentia and Australia. *Geology* 28, 103–106.
- Cande, S.C., Mutter, J.C., 1982. Revised identification of the oldest seafloor spreading anomalies between Australia and Antarctica. *Earth and Planet. Sci. Lett.* 58, 151–160.
- Cawthorn, R., Collerson, K.D., 1974. The recalculations of pyroxene end-member parameters and the estimation of ferrous and ferric iron content from electron microprobe analyses. *American Mineralogist* 59, 1203–1208.

- Coleman, R.G., Lee, D.E., Beatty, L.B., Brabcock, W.W., 1965. Eclogites and eclogites: their differences and similarities. *Geol. Soc. of Am. Bull.* 76, 483–508.
- Compston, W., Williams, I.S., Kirschvink, J.L., Zhang, Z., Ma, G., 1992. Zircon U–Pb ages for the Early Cambrian time-scale. *J. of the Geol. Soc. of Lond.* 149, 171–184.
- Cuthbert, S.J., Carswell, D.A., 1990. Formation and exhumation of medium-temperature eclogites in the Scandinavian Caledonides. In: Carswell, D.A. (Ed.), *Eclogite facies rocks*. Chapman and Hall, New York, pp. 180–203.
- Daly, S.J., Fanning, C.M., Fairclough, M.C., 1998. Tectonic evolution and exploration potential of the Gawler Craton, South Australia. *AGSO Journal of Australian Geology and Geophysics* 17, 145–168.
- Dalziel, I.W.D., 1991. Pacific margins of Laurentia and East Antarctica–Australia as a conjugate rift pair: Evidence and implications for an Eocambrian supercontinent. *Geology* 19, 598–601.
- Damaske, D., 1990. Technical description of the 1:250 000 maps of the anomalies of the Total Magnetic Field, Lower Rennick Glacier, North Victoria Land, Antarctica: Aeromagnetic survey during the expedition GANOVEX V 1988/1989. Bundesanstalt für Geowissenschaften und Rohstoffe, Hanover.
- Fanning, C.M., Flint, R.B., Parker, A.J., Ludwig, K.R., Blissett, A.H., 1988. Refined Proterozoic evolution of the Gawler Craton, South Australia, through U–Pb zircon geochronology. *Precambrian Res.* 40/41, 363–386.
- Fanning, C.M., Daly, S.J., Bennett, V.C., Menot, R.P., Peucat, J.J., Oliver, R.L., Monnier, O., 1995. The ‘Mawson Block’: once contiguous Archaean to Proterozoic crust in the East Antarctic shield and Gawler Craton. VII International Symposium on Antarctic Earth Sciences, Siena, Italy, p. 124.
- Fanning, C.M., Moore, D.H., Bennett, V.C., Daly, S.J., 1996. The ‘Mawson Continent’: Archean to Proterozoic crust in the East Antarctic Shield and Gawler Craton, Australia: A cornerstone in Rodinia and Gondwanaland. *Geol. Soc. of Aust.*, 14th Aust. Geol. Conv. 41, 135.
- Finn, C.A., Damaske, D., Mackey, T., Moore, D., 1998. The aeromagnetic connection: a new look at the Gondwana Geology of Antarctica and Australia. *Geol. Soc. of Aust.*, 16th Aust. Geol. Conv. 49, 145.
- Flodin, E.A., Wooden, J.L., Miller, D.M., Barth, A.P., Bone, J.D., 1997. Petrogenesis of early Proterozoic granitic and meta-granitic rocks in the Mojave Crustal Province, Southern California. *Geol. Soc. of Am. Abstr. with Programs* 29, 13.
- Gebauer, D., 1990. Isotopic systems — geochronology of eclogites. In: Carswell, D.A. (Ed.), *Eclogite Facies Rocks*. Chapman and Hall, New York, pp. 141–159.
- Gebauer, D., Grunfelder, M., 1979. U–Pb zircon and Rb–Sr mineral dating of eclogites and their country rocks. Example: Munchberg gneiss massif, Northeast Bavaria. *Earth and Planet. Sci. Lett.* 42, 35–44.
- Goodge, J.W., Borg, S.G., Smith, B.K., Bennett, V.C., 1991. Tectonic significance of Proterozoic ductile shortening and translation along the Antarctic margin of Gondwana. *Earth and Planet. Sci. Lett.* 104, 116 see also erratum, 102, 58–70.
- Goodge, J.W., Dallmeyer, R.D., 1992. $^{40}\text{Ar}/^{39}\text{Ar}$ mineral age constraints on the Paleozoic tectonothermal evolution of high-grade basement rocks within the Ross Orogen, central Transantarctic Mountains. *J. of Geol.* 100, 91–106.
- Goodge, J.W., Dallmeyer, R.D., 1996. Contrasting thermal evolution within the Ross Orogen, Antarctica: Evidence from mineral $^{40}\text{Ar}/^{39}\text{Ar}$ ages. *J. of Geol.* 104, 435–458.
- Goodge, J.W., Fanning, C.M., 1999. 2.5 billion years of punctuated Earth history as recorded in a single rock. *Geology* 27, 1007–1010.
- Goodge, J.W., Hansen, V.L., Peacock, S.M., 1992. Multiple petro-tectonic events in high-grade metamorphic rocks of the Nimrod group, central Transantarctic Mountains, Antarctica. In: Yoshida, Y., Kaminuma, K., Shiraishi, K. (Eds.), *Recent Progress in Antarctic Earth Science*. Terra Scientific, Tokyo, pp. 203–209.
- Goodge, J.W., Hansen, V.L., Peacock, S.M., Smith, B.K., Walker, N.W., 1993a. Kinematic evolution of the Miller Range shear zone, central Transantarctic Mountains, Antarctica, and implications for Neoproterozoic to early Paleozoic tectonics of the East Antarctic margin of Gondwana. *Tectonics* 12, 1460–1478.
- Goodge, J.W., Walker, N.W., Hansen, V.L., 1993b. Neoproterozoic–Cambrian basement-involved orogenesis within the Antarctic margin of Gondwana. *Geology* 21, 37–40.
- Griffin, W.L., Austrheim, H., Brastad, K., Bryhni, I., Krill, A.G., Krogh, E.J., Mork, M.B.E., Qvale, H., Torudbakken, B., 1985. High-pressure metamorphism in the Scandinavian Caledonides. In: Gee, D.G., Sturt, B.A. (Eds.), *The Caledonide Orogen — Scandinavia and Related Areas*. Wiley, New York, pp. 783–801.
- Grindley, G.W., 1972. Polyphase deformation of the Precambrian Nimrod Group, central Transantarctic Mountains. In: Adie, R.J. (Ed.), *Antarctic Geology and Geophysics*. Universitetsforlaget, Oslo, pp. 313–318.
- Grindley, G.W., Laird, M.G., 1969. Geology of the Shackleton Coast, Antarctica. In: Bushnell, V.C., Craddock, C. (Eds.), *Geologic Map of Antarctica, Antarctic Map Folio Series, Folio 12, Sheet 15*. American Geographical Society, New York.
- Grindley, G.W., McDougall, I., 1969. Age and correlation of the Nimrod Group and other Precambrian rock units in the central Transantarctic Mountains, Antarctica. *N. Z. J. of Geol. and Geophys.* 12, 391–411.
- Grindley, G.W., McGregor, V.R., Walcott, R.I., 1964. Outline of the geology of the Nimrod–Beardmore–Axel Heiberg Glaciers region, Ross Dependency. In: Adie, R.J. (Ed.), *Antarctic Geology*. North-Holland, New York, pp. 206–218.
- Gunner, J., Mattinson, J.M., 1975. Rb–Sr and U–Pb isotopic ages of granites in the central Transantarctic Mountains. *Geol. Mag.* 112, 25–31.

- Gunner, J.D., 1969. Petrography of metamorphic rocks from the Miller Range, Antarctica. Ohio State University, Columbus, OH, Institute of Polar Studies Report No. 32.
- Gunner, J.D., 1976. Isotopic and geochemical studies of the pre-Devonian basement complex, Beardmore Glacier region, Antarctica. Ohio State University, Columbus, Institute of Polar Studies Report No. 41.
- Gunner, J.D., 1983. Basement geology of the Beardmore Glacier region. In: Turner, M.D., Spletstoesser, J.F. (Eds.), *Geology of the Central Transantarctic Mountains*. American Geophysical Union, Washington, DC, Antarctic Research Series, vol. 36, pp. 1–9.
- Hoffman, P.F., 1991. Did the break of Laurent. turn Gondwanaland inside-out? *Science* 252, 1409–1412.
- Krogh, T.E., Mysen, B.O., Davis, G.L., 1974. A Paleozoic age for the primary minerals of a Norwegian eclogite. *Carnegie Inst. of Wash. Year Book* 73, 575–576.
- Ludwig, K.R., 1999. User's manual for Isoplot/Ex, Version 2.10, A geochronological toolkit for Microsoft Excel. Berkeley Geochronology Center, Berkeley, CA, Special Publication No. 1a.
- Messiga, B., Tribuzio, R., Vannucci, R., 1990. Mafic and ultramafic pods with eclogite relics from the Proterozoic Nagsugtoqidian mobile belt of east Greenland. *Lithos* 25, 101–118.
- Moore, E.M., 1991. Southwest U.S.–East Antarctica (SWEAT) connection: A hypothesis. *Geology* 19, 425–428.
- Morimoto, N., Fabries, J., Ferguson, A.K., Ginzburg, I.V., Ross, M., Seifert, F.A., Zussman, J., Aoki, K., Gottardi, G., 1988. Nomenclature of pyroxenes. *Am. Mineral.* 73, 1123–1133.
- Muir, R.J., Ireland, T.R., Weaver, S.D., Bradshaw, J.D., 1996. Ion microprobe dating of Paleozoic granitoids: Devonian magmatism in New Zealand and correlations with Australia and Antarctica. *Chem. Geol.* 127, 191–210.
- Mysen, B.O., Heier, K.S., 1972. Petrogenesis of eclogites in high grade metamorphic gneisses, exemplified by the Hareidland eclogite, western Norway. *Contrib. to Mineral. and Petrol.* 36, 73–94.
- Nelson, D.R., Myers, J.S., Nutman, A.P., 1995. Chronology and evolution of the Middle Proterozoic Albany–Fraser Orogen, Western Australia. *Aust. J. of Earth Sci.* 42, 481–495.
- Oliver, R.L., Cooper, J.A., Truelove, A.J., 1983. Petrology and zircon geochronology of Herring Island and Commonwealth Bay and evidence for Gondwana reconstruction. In: Oliver, R.L., James, P.R., Jago, J.B. (Eds.), *Antarctic Earth Science*. Australian Academy of Science, Canberra, pp. 64–68.
- Oliver, R.L., Fanning, C.M., 1997. Australia and Antarctica: Precise correlation of Palaeoproterozoic terrains. In: Ricci, C.A. (Ed.), *The Antarctic Region: Geological Evolution and Processes*. Terra Antarctica Publication, Siena, pp. 163–173.
- Paces, J.B., Miller, J.D., 1993. Precise U–Pb ages of Duluth Complex and related mafic intrusions, northeastern Minnesota: Geochronological insights to physical, petrogenic, paleomagnetic, and tectonomagmatic processes associated with the 1.1 Ga Midcontinent Rift System. *J. of Geophys. Res.* 98, 13997–14013.
- Paquette, J., Menot, R., Peucat, J., 1989. REE, Sm–Nd and U–Pb zircon study of eclogites from the Alpine External Massifs (Western Alps): evidence for crustal contamination. *Earth and Planet. Sci. Lett.* 96, 181–198.
- Parker, A.J., 1993. Geological framework. In: Drexel, J.F., Preiss, W.V., Parker, A.J. (Eds.), *The Geology of South Australia*, vol. 1, Precambrian. Geological Survey of South Australia Bulletin, vol. 54, Chapter 2, pp. 9–32.
- Peacock, S.M., Goodge, J.W., 1995. Eclogite-facies metamorphism preserved in tectonic blocks from a lower crustal shear zone, central Transantarctic Mountains, Antarctica. *Lithos* 36, 12–13.
- Peucat, J.J., Menot, R.P., Fanning, C.M., 1999. The Terre Adélie Basement in the East-Antarctica Shield: geological and isotopic evidence for a major 1.7 Ga thermal event; comparison with Gawler Craton in South Australia. *Precambrian Res.* 94, 205.
- Peucat, J.J., Vidal, Ph., Godard, G., Postaire, B., 1982. Precambrian U–Pb zircon ages in eclogites and garnet pyroxenites from South Brittany (France): an old oceanic crust in the West European Hercynian belt? *Earth and Planetary Science Letters* 60, 70–78.
- Ross, G.M., Parrish, R.R., Winston, D., 1992. Provenance and U–Pb geochronology of the Mesoproterozoic Belt Supergroup (northwestern United States): Implications for age of deposition and pre-Panthalassa plate reconstructions. *Earth and Planet. Sci. Lett.* 113, 57–76.
- Rubatto, D., Gebauer, D., Compagnoni, R., 1999. Dating of eclogite-facies zircons: the age of Alpine metamorphism in the Sesia–Lanzo Zone (Western Alps). *Earth and Planet. Sci. Lett.* 167, 141–158.
- Schaltegger, U., Fanning, C.M., Gunther, D., Maurin, J.C., Schlumann, K., Gebauer, D., 1999. Growth, annealing and recrystallization of zircon and preservation of monazite in high-grade metamorphism: conventional and in-situ U–Pb isotope, cathodoluminescence and microchemical evidence. *Contrib. to Mineral. and Petrol.* 134, 186–201.
- Sheraton, J.W., Black, L.P., Tindle, A.G., 1992. Petrogenesis of plutonic rocks in a Proterozoic granulite-facies terrane — the Bunge Hills, East Antarctica. *Chem. Geol.* 97, 163–198.
- Sheraton, J.W., Oliver, R.L., Stuwe, K., 1989. Geochemistry of Proterozoic amphibolite dykes of Commonwealth Bay, Antarctica, and possible correlations with mafic dyke swarms elsewhere in Gondwanaland. *Precambrian Res.* 44, 353–361.
- Sheraton, J.W., Tingey, R.J., Black, L.P., Oliver, R.L., 1993. Geology of the Bunge Hills area, Antarctic: implications for Gondwana correlations. *Antarc. Sci.* 5, 85–102.
- Tera, F., Wasserburg, G.J., 1972. U–Th–Pb systematics in three Apollo 14 basalts and the problem of initial Pb in lunar rocks. *Earth and Planet. Sci. Lett.* 14, 281–304.
- Tingey, R.J., 1991. The regional geology of Archaean and Proterozoic rocks in Antarctica. In: Tingey, R.J. (Ed.), *The*

- geology of Antarctica. Clarendon Press, Oxford. Oxford Monograph on Geology and Geophysics, vol. 17, pp. 1–73.
- Van Schmus, W.R., Bickford, M.E., Condie, K.C., 1993. Early Proterozoic crustal evolution. In: Reed, J.C., et al. (Eds.), *Precambrian: Conterminous U.S. DNAG* vol. C-2. The Geological Society of America, Boulder, CO, pp. 270–281.
- Vavra, G., 1990. On the kinematics of zircon growth and its petrogenetic significance: a cathodoluminescence study. *Contrib. to Mineral. and Petrol.* 106, 90–99.
- Walker, N.W., Goodge, J.W., 1991. Significance of Late Archean–Early Proterozoic U–Pb ages of individual Nimrod Group detrital zircons and Cambrian plutonism in the Miller Range, Transantarctic Mountains. *Geol. Soc. of Am. Abstr. with Programs* 23, 306.
- Webb, A.W., Thomson, B.P., Blissett, A.H., Daly, S.J., Flint, R.B., Parker, A.J., 1986. Geochronology of the Gawler Craton, South Australia. *Aust. J. of Earth Sci.* 33, 119–143.
- Williams, I.S., 1998. U–Th–Pb geochronology by ion microprobe. In: McKibben, M.A., Shanks III, W.C., Ridley, W.I. (Eds.), *Applications of Microanalytical Techniques to Understanding Mineralizing Processes, Reviews in Economic Geology*, vol. 7, pp. 1–35.
- Williams, I.S., Compston, W., Collerson, K.D., Arriens, P.A., Lovering, J.F., 1983. A reassessment of the age of the Windmill Metamorphics, Casey area. In: Oliver, R.L., James, P.R., Jago, J.B. (Eds.), *Antarctic Earth Science*. Australian Academy of Science, Canberra, pp. 73–76.
- Wooden, J.L., Miller, D.M., 1990. Chronologic and isotopic framework for Early Proterozoic crustal evolution in the eastern Mojave Desert region. *J. of Geophys. Res.* 95, 20133–20146.